

**THE BEHAVIOR OF TaC AND TaC+Al ELECTRODES IN TiCl<sub>4</sub>  
PLASMA GASES**

---

**A  
THESIS  
BY**

Yong Gao

Department of Chemical Engineering -- McGill University

Under the supervision of Dr. R. J. Munz and Dr. P. Tsantrizos

Submitted to the Faculty of Graduate Studies and Research of McGill  
University in partial fulfillment of the requirements for the degree of  
Master of Engineering

McGill University  
Montreal, Canada

December 1990

*To my parents and my sister's family*

## ACKNOWLEDGEMENTS

---

My sincere appreciation is expressed to my supervisors Dr. R. J. Munz and Dr. P. Tsantrizos for their guidance and help throughout all the phases of this work.

Special thanks to G. LeBlanc, Dr. R. N. Szente, Dr. K. Shanker, G. Q. Chen and M. Habelrih for their friendly help,

and to the plasma group supervisors: Dr. D. Berk, Dr. J. L. Meunier, and Dr. W. Gauvin for their valuable input.

A lot thanks to Mr. J. Dumont, Mr. A. Krish, Mr. A. Gagnon, Mr. D. Leishman and Mr. C. Dolan, Mr. L. Cusmich, and Mr. N. Habib for all their great assistance.

To the plasma group member: Murray, Bogdan, Muftah, Mario, Chico, Mike, and to my fiends: Yonghao, Jian, Biao, Lijie and many others, thank all of them very much.

Many thanks to P. Fong, Mrs. A. Prihoda, Louise Miller and Valerie Hubbard for their help.

## Abstract

---

An experimental study was carried out to identify a suitable electrode material for the treatment of  $\text{TiCl}_4$  in a plasma arc. The behavior of the arc voltage, velocity and rate of electrode erosion were examined in a DC plasma torch using concentric cylindrical electrodes and arc rotation by an axial magnetic field. The results of the experiments and analyses showed that pure TaC was not suitable as an electrode material because of its mechanical failure under thermal stress. A new composite material, TaC infiltrated with Al proved to be successful.

Stable plasmas were produced containing up to 30 % titanium tetrachloride in argon at a current of 100 amperes, an interelectrode gap of 4 mm, and a magnetic field strength of 1000 Gauss. The cathode erosion rate was less than 30 micrograms/C at a titanium tetrachloride concentration of 14.3 %.

# CONTENTS

---

Abstract	
Resume	
Acknowledgement	
Contents	1
List of Figures	5
List of Tables	7
<b>Chapter 1. Introduction</b>	
1.1 Background Information	8
1.2 Objectives	10
<b>Chapter 2. Literature Review</b>	
2.1 Plasma Phenomena	
A. The Definition of Plasmas	13
B. Categories of Plasma	14
2.2 The Approaches to Producing Plasmas	
A. Plasma Generation	14
B. Electrical Discharge	15
2.3 Plasma Devices	
A. Electrodeless Devices	19
B. Electrode Devices	20
2.4 Phenomena of Electrode Erosion	
A. Introduction	25
B. Parameters Affecting Electrode Erosion	25

## Resumé

Une étude expérimentale fut entreprise afin d'identifier un matériau d'électrode permettant le traitement de  $TiCl_4$  dans un plasma d'arc. Le comportement de la tension et de la vitesse de rotation de l'arc ainsi que du taux d'érosion de l'électrode ont été étudiés sur une torche à plasma munie d'électrodes cylindriques concentriques. Un champ magnétique axial imposait une rotation de l'arc entre les électrodes. Les résultats expérimentaux indiquent qu'une cathode de TaC pure ne peut supporter les stress thermiques, provoquant ainsi une défaillance mécanique rapide de l'électrode. Un nouveau matériau composite formé de TaC avec infiltration d'aluminium a été développé et testé avec succès comme matériau d'électrode.

Des plasmas stables ont été produits avec des pourcentages allant jusqu'à 30% de tetrachlorure de titane dans l'argon à un courant d'arc de 100 ampères, un espacement interélectrodes de 4 mm et un champ magnétique de 1000 Gauss. Le taux d'érosion de la cathode mesuré à une concentration de tetrachlorure de titane de 14.3% était inférieur à  $30 \times 10^{-6}$  g/C.

C.	Improvement of Electrode Erosion	26
2.5	Plasma Containing $TiCl_4$	28
<b>Chapter 3. Experimental Apparatus</b>		
3.1	Introduction	33
3.2	The DC-Plasma Arc Torch	33
A.	The Configuration of the Electrodes	36
B.	The Extension of the Reactor	36
C.	The Viewing Window	38
D.	The Relocation of the Optical Fiber	38
E.	Plasma Gas Feed Lines	38
3.3	The Feeding System	38
3.4	The Scrubbing System	39
3.5	The Heating/Cooling System	42
3.6	The Data Recording System	42
3.7	Power Supplies	43
3.8	The High Frequency Unit	43
<b>Chapter 4 Experimental Procedures</b>		
4.1	Introduction	44
4.2	Preparation of Experiments	
A.	Preparation of Electrode	44
B.	Cleaning Procedure of the system	45
C.	Assembling Procedure	45
D.	Pre-Check Procedure	45
4.3	Operation of Experiments	
A.	Starting Procedure	46

	B. Operating of Tests	46
4.4	Post-Treatments	47
<b>Chapter 5 Pioneering Analysis</b>		
5.1	Thermodynamic Considerations	
	A. Basic Thermodynamic Analysis	48
	B. Conclusion	51
5.2	Preliminary Experiments	
	A. Preparation of Pure TaC Cathode Rings	51
	B. Experimental Conditions	55
	C. Results of Experiments	55
5.3	Basic Failure Analysis	
	A. Temperature Cycling and Gradient	60
	B. Thermo-Mechanical Failure of the Electrode Ring	61
	C. Conclusion	62
<b>Chapter 6 Experiments with TaC+Al Electrodes</b>		
6.1	The Preparation of TaC+Al Electrodes	
	A. Fabrication of TaC+Al Electrode	63
	B. The Properties of TaC+Al Material	63
6.2	TaC+Al Electrode in Argon Plasma Gas	
	A. Results	66
	B. Discussion	66
6.3	TaC+Al Electrodes in $TiCl_4$ + Argon Plasma Gases	
	A. Experimental Conditions	70
	B. The Features of the Arc Voltage	70
	C. Weight Loss and Erosion Rate	75

D. Arc Velocity	83
E. Effect of Arc Velocity on Erosion Rate	89
F. SEM Analysis	91
G. The Behavior of the Anodes	97
H. Conclusions	98
<b>Chapter 7 Conclusions and Recommendations</b>	
7.1 Conclusions	100
7.2 Recommendations	101
<b>References</b>	102

## LIST OF FIGURES

---

<b>Figures</b>	<b>Caption</b>	
i-1	Titanium Production - the Kroll Process	11
2-1	Voltage vs. Current for Neon at 40 mm Hg	16
2-2	Characteristics of Arc Discharges	18
2-3	Schematic Drawing of RF Plasma Torch	20
2-4	Schematic Drawing of Transferred Arc Torch	22
2-5	Schematic Drawing of DC Plasma Torch	24
2-6	Arc Voltage Variations with Time for $TiCl_4$ -Rich Arcs Using a Thoriated Tungsten Cathode	31
2-7	Arc Voltage Variations with Time for $TiCl_4$ -Rich Arcs Using a Thoriated Tantalum Carbide Cathode	32
3-1	Schematic Drawing of the Overall Experimental Set-up	34
3-2	Schematic Drawing of the Reactor Assembly	35
3-3	Schematic Drawing of the Anode and the Cathode	37
3-4	Schematic Drawing of the Feeding System	40
3-5	Schematic Drawing of the Scrubbing System	41
5-1	The Flow Chart of Fabricating TaC Cathode Ring	53
5-2	The Rings in Different Stages of Fabrication	54
5-3	The Microstructure of the Ring (SEM)	55
5-4	The Photograph of a Cathode Ring and a Copper Anode After Testing	58
5-5	The Fractured Parts of the Pure TaC Cathode Ring	59
6-1	The Flow Chart of TaC+Al Electrodes Fabrication	64
6-2	The Micrograph of a TaC+Al Electrode	65
6-3	The Photograph of a Ring and a Tip After a One Hour Test	69
6-4	The Microstructure of TaC+Al After a One Hour Test	69

6-5	Average Arc Voltage vs the Concentration of $\text{TiCl}_4$	72
6-6	The Features of Average Voltage vs Operating Time	74
6-7	The Response of Voltage During 14% $\text{TiCl}_4$ Gas Testing	76
6-8	The Weight Loss of TaC+Al Cathode in $\text{TiCl}_4$ Plasma	79
6-9	The Weight Loss of TaC+Al Cathode vs the Concentration of $\text{TiCl}_4$	80
6-10	The Erosion Rate of TaC+Al Cathode in $\text{TiCl}_4$ Plasma	82
6-11	Erosion Rate as a Function of $\text{TiCl}_4$ Concentration at Different Times	84
6-12	Arc Velocity vs $\text{TiCl}_4$ Concentration	86
6-13	Arc Velocity as a Function of $\text{TiCl}_4$ Concentration	88
6-14	Effect of Arc Velocity on Erosion Rate of Electrodes	90
6-15	The Micrograph of the Cathode Inside Surface	92
6-16	The Micrograph of the Cathode Outside Surface	93
6-17	The Comparison of Element Mapping on the Cathode Surface	94
6-18	The Deposits of Titanium on the Cathode Surface	95
6-19	The Analysis of the Composition on the Cathode Surface	96
6-20	A Tantalum Carbide Anode Tip After Testing	99
6-21	A Photograph of the Arc in $\text{TiCl}_4$ Gas	99

## LIST OF TABLES

---

<b>Tables</b>	<b>Caption</b>	
1-1	Economics of Titanium Production	9
2-1	Experimental Data on Cathode Erosion	30
5-1	The Results of Chemical Reaction Analysis	50
5-2	The Results of Equilibrium Analysis at 2000 K	50
5-3	The Composition of TaC Powder	52
5-4	The Experimental Conditions	57
6-1	The Properties of TaC+Al Material	65
6-2	Experimental Conditions for TaC+Al Electrodes in Argon Plasma	67
6-3	The Results of TaC+Al Cathode Rings in Argon Gas	68
6-4	Operating Conditions for $\text{TiCl}_4$ + Argon Plasma Gases	70
6-5	The Arc Voltage vs $\text{TiCl}_4$ Concentration	71
6-6	Reproducibility of the Arc Voltage	73
6-7	Weight Loss and Erosion Rate of Electrodes	77
6-8	The Arc Velocities in Different Conditions	85

# CHAPTER 1.

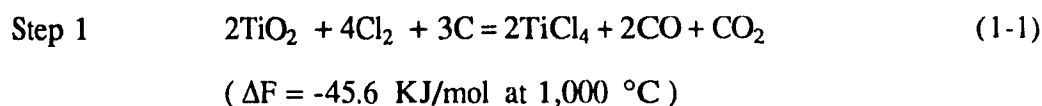
## INTRODUCTION

---

### 1.1 Background Information

Since the beginning of the titanium industry about forty years ago the different approaches to titanium production have attracted a great deal of attention as the metal is still relatively expensive, and its excellent properties are producing a greater demand. Though some successful methods were developed, for example, the Kroll and Hunter (1910) processes have increased titanium production, the applications of titanium are still limited by the high production cost and severe operating problems associated with its production. Table 1-1 (Tsantrizos, 1988) gives a brief survey of the cost profile of producing titanium. Over 60% of the cost of titanium are attributed to the consolidation of the sponge into dense metal and the forming of mill products, and only 4% of the total cost is spent in the treatment of the ore. Reductions in production costs would greatly increase the applications of titanium in areas where its properties are desirable.

The present common approaches of titanium production are generally based on the following chemical reactions which are first chlorinating titanium oxide (rutile) to titanium tetrachloride and then reducing the chloride to the metal:



Step 2.

A. the Hunter process:



Table 1-1. Economics of Titanium Production

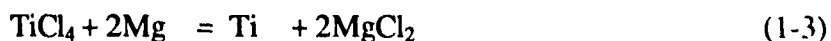
Compound	Price (US\$/kg)	Value of Contained Ti (US\$/kg)	% of Titanium Metal Price
TiO <sub>2</sub> (rutile ore)	0.56 *	0.93	4
TiCl <sub>4</sub> (tech.bulk)	0.66 **	2.61	12
Ti sponge(99.3%)	9.13 ***	9.19	43
Ti metal (com.pure)	21.45 ***	21.45	100

Note: \* effective: Sept. 1986 Engineering and Mining Journal  
 \*\* effective: Oct. 1986 Chemical Marketing Reporter  
 \*\*\* effective: Oct. 1986 American Metal Market

Ref. Tsantrizos, 1988

$$(\Delta F = -946,420 + 65.2 T \text{ J/mol, } T \text{ in K})$$

### B. the Kroll process



$$(\Delta G = -321,954 \text{ J/mol at } 1,273 \text{ K})$$

A simplified flow chart of the process is shown in Figure 1-1 (Tsantrizos, 1988).

Either the Hunter or the Kroll process produces titanium sponge which must be first separated from the respective chlorides and then consolidated to its valuable dense metal form. The cost and operating difficulties associated with both the Hunter and the Kroll processes have pushed workers to search for alternative methods of producing the metal. Some of these methods involve the direct reduction of titanium dioxide to the metal. Others have proposed an electrolytic process using a bath of fused salts to reduce titanium tetrachloride to titanium metal. (Barksdale, 1966, and Ikeshima, 1985).

A process which involves the direct reduction of  $\text{TiCl}_4$  to the metal in high temperature plasmas has been proposed for years. The basic idea in this process is to thermally dissociate the titanium tetrachloride molecule into its monoatomic constituents and capture the titanium before it recombines with chlorine. Some contributions have been made (Harnish, Heymer and Schallus, 1963, Miller and Ayen, 1968, Tsantrizos, 1988), but there are still certain critical problems in this process to be solved. One of them is the target of this study.

## 1.2 Objectives

The present work will be specifically concerned with the problems of identifying an electrode material which is compatible with titanium tetrachloride plasma and developing a stable titanium tetrachloride plasma over prolonged periods. The erosion of such electrodes is expected to be one of the major concerns.

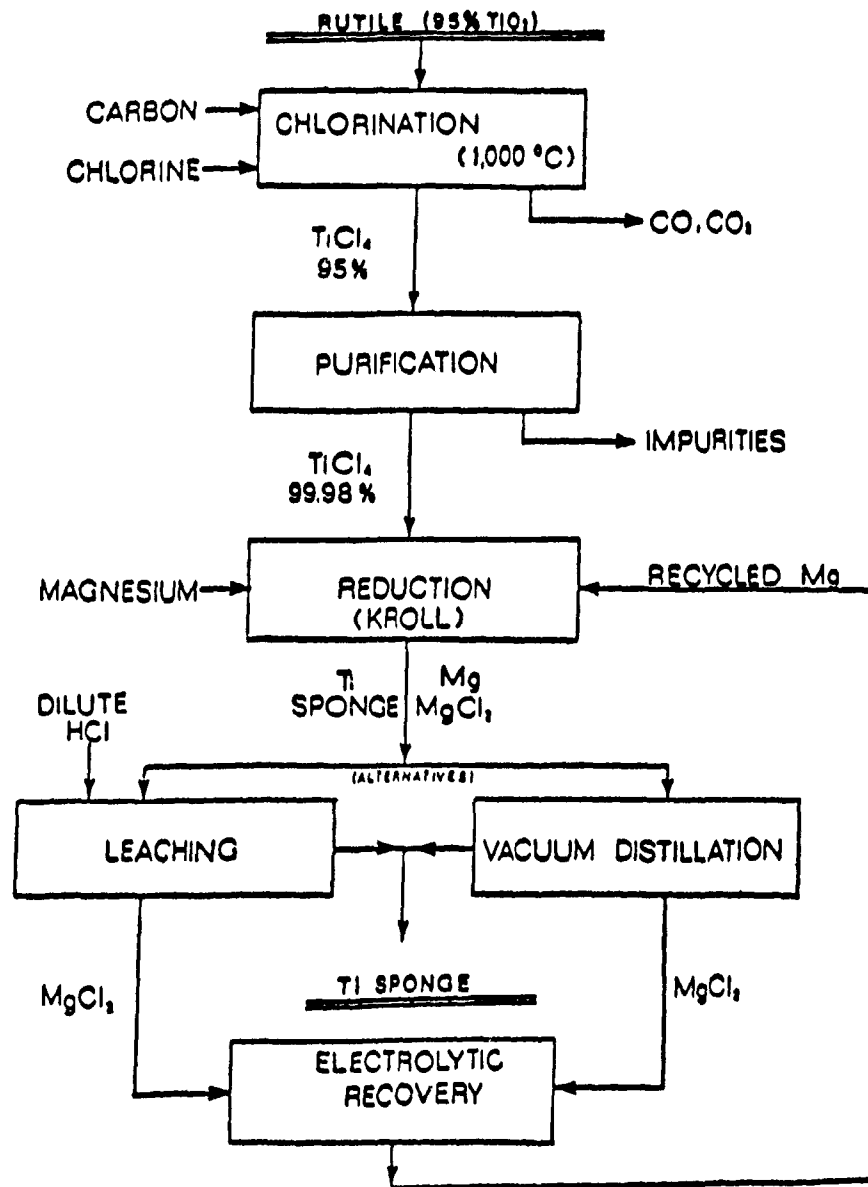


Figure 1-1 Titanium Production - the Kroll Process

The originally proposed electrode material was TaC but the feasibility of using other materials was also examined. A composite material of TaC+Al was found to be most promising.

This thesis consists of seven chapters. Chapters 1 and 2 briefly review the background of this project, plasma technology and the relevant literature of  $TiCl_4$  plasma research. In chapters 3 and 4 the equipment and experimental procedures are described. The pioneering tests with pure TaC and relevant discussion are given in chapter 5. Chapter 6 discusses the results of the experiments with TaC+Al. A short summary and conclusions with recommendations are presented in chapter 7.

## CHAPTER 2.

### LITERATURE REVIEW

---

#### 2.1 Plasma Phenomena

Plasmas and their generation have been thoroughly reviewed by Guile (1971 and 1984), Munz (1974), Mehmetoglu (1980) and Szente (1986); here only the most important points will be discussed.

##### A. Definition of Plasma

A plasma is a conglomeration of positively and negatively charged and neutral particles. It is on the average neutral, because the number density of the positive charges is equal to that of the negative ones. The plasma contains two or more kinds of charge carriers: free electrons and positive ions. Sometimes it also has negative ions and more than one kind of positive ion. The ions may be singly charged or multiply charged; they may also be atomic or molecular.

The plasma state is the fourth state of matter: adding sufficient energy to a gas makes a plasma. The energy added is partly converted into random translational (and in the case of molecules rotational and vibrational) energy and partly into dissociation and ionization energy. The physical and chemical properties of a plasma are different from those of the other three states (solid, liquid, and gas) of matter. Because of its electrical conductivity, plasma can interact with electric and magnetic fields.

The plasma state is by far the most common form of matter. Up to 99 percent of the matter in the universe exists in the plasma state. It is also the most energetic state; a body will require on average  $10^{-2}$  eV ( $1\text{eV} = 1.602 \times 10^{-19}$  J) per particle to change its state from solid to liquid or from liquid to gas, whereas a change of state from gas to

plasma will require from 1 to 30 eV per particle, depending on the materials ( Kettai and Hoyaux, 1973).

#### B. Categories of Plasma

Plasmas they can be generally classified into two types:

i) Cold plasmas including dark discharges. These plasmas carry currents from  $10^{-6}$  to  $10^{-1}$  A, and are often formed under low pressure ( for example neon and fluorescent lamps ).

ii) Hot or thermal plasmas, which operate at or above atmospheric pressures and carry current higher than one ampere (for example, plasma spraying torches) In these plasmas local thermodynamic equilibrium (LTE) often exists among the electrons, ions and atoms. The typical temperature range of thermal plasmas is between 2,500 and 30,000 K or higher, with ionization levels greater than 0.1 percent (Howartson, 1976). A more detailed discussion will be presented in the following section.

## 2.2 The Approaches to Producing Plasmas

#### A. Plasma Generation

Plasmas may be generated by many ways, such as:

i) Electrical Discharge: This is the major method and is used in our project. It will be discussed in more detail in the following pages;

ii) Thermal Ionization: At very high temperature a proportion of molecules in a gas will get enough energy to excite and ionize other molecules with their collisions. Consequentially a plasma is produced

iii) Shock Waves

iv) Nuclear Reaction

v) Irradiation by Alpha or Gama Rays

## vi) Chemical Reactions of High Specific Energy

### B. Electrical Discharge

This is by far the most important method used to produce plasma. It can be classified as *Electrodeless Discharge*, such as capacitive or inductive coupling, and *Electrode Discharge* of four types which is most concerned in our study and will be discussed below.

From Figure 2-1 (Francis,1956) we can divide the whole range of voltage - current of electrical discharges into four regions which are:

#### i) Townsend (Dark) Discharge

This is a kind of dark or low pressure plasma, produced in the region B-C of Figure 2-1. Townsend discharge carries currents up to  $10^{-5}$  A, the voltages are relatively high.

#### ii) Corona

Corona is identified as a kind of cold electrical discharge in the  $V-I$  range of 1-100kV and  $10^{-5}$  to  $10^{-4}$  A, shown in Figure 2-1 the region C-D.

#### iii) Glow Discharge

With increasing current, the characteristics of the discharge will be changed. In Figure 2-1 from D section to G section it is found that the voltage will change as the current increases, and the changing ranges are often divided into several subregions: such as subnormal; normal, and abnormal depending on the range of the current, from around  $10^{-4}$  to 1 A.

#### iv) Arc Discharge

An arc is also a specific form of a discharge of electricity produced in a certain medium, such as a gas or a vapor etc., between two electrodes, and it can be initiated by several techniques which are classified as the separation of current-carrying contacts; the melting and vaporization of thin wires; transition from a glow discharges

shown as in Figure 2-1; or transition and follow-through of an impulse or high-frequency spark breakdown which is the means used in our research.

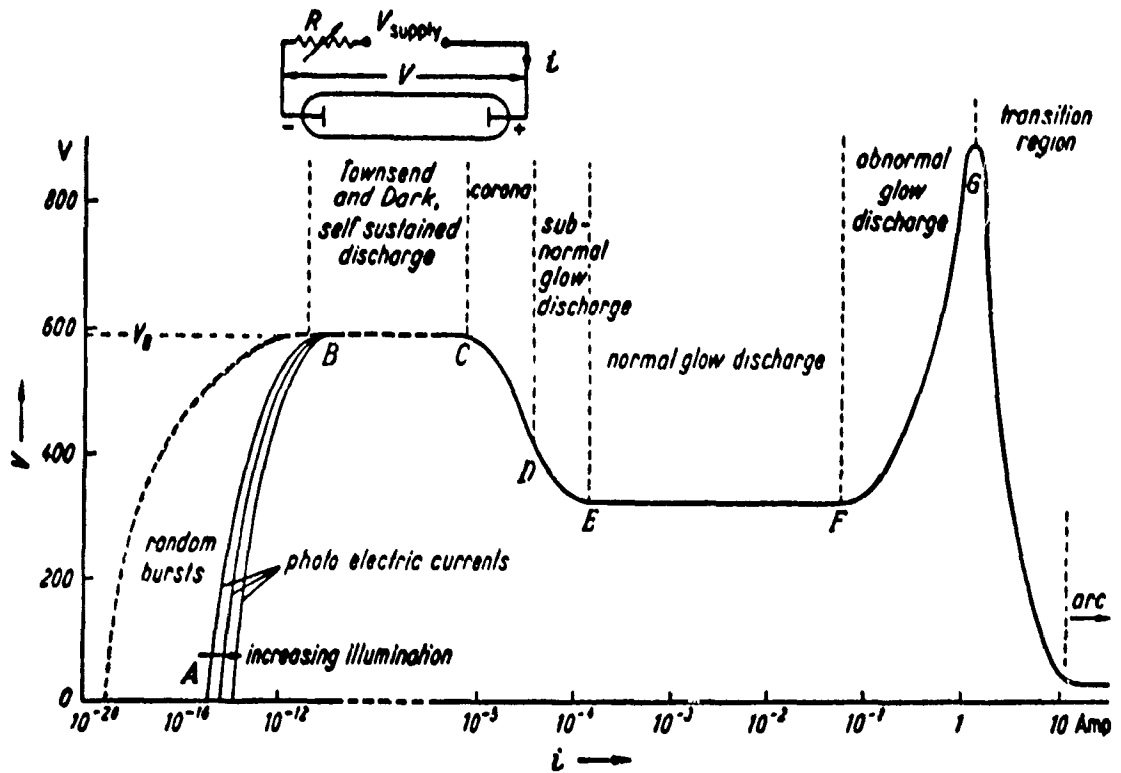


Figure 2-1. Voltage vs Current for Neon at 40 mm Hg

All kinds of arcs have the some similar features, i.e. the conducting gases between the electrodes have high temperature ( $>4000$  K) and high luminosity. The whole arc "burning" in the gap between the electrodes may be divided into three regions:

*- The Positive Column*

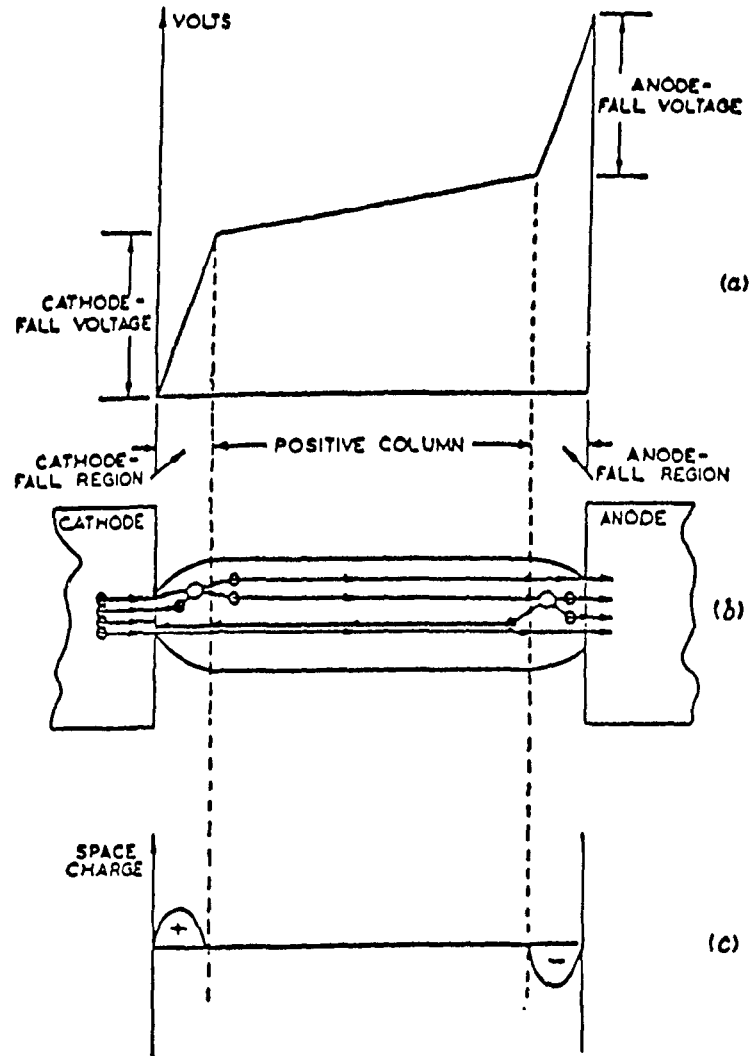
The positive column is the main body of the arc which acts as a normal electrical conductor and has a relatively low potential gradient which may be as low as 10V/cm and is unlikely to exceed about 100V/cm (Guile, 1971). Figure 2-2 shows schematically the distributions in the arc (Edels, 1961). It has been shown experimentally that the field strength is constant for a cylindrically symmetric column and in all column configurations. From Poisson's law, the net space-charge should be zero, meaning that the plasma will be neutral.

*- The Cathode-Fall Region*

For current continuity, electrons must be emitted from the solid cathode into the plasma column. There are different theories, such as thermionic emission and field emission etc., to describe the mechanism of emission of the electrons from cathodes. The cathode potential fall for an arc is relatively lower (10-20V) than that for a glow discharge ( $>100$ V). This region is very sensitive to the properties of the cathode material and gas, and their interaction.

*- The Anode-Fall Region*

From the Figure 2-2 it is observed that the anode region also has a potential fall due to a high concentration of electrons rushing to the surface of the anode. Because the current continuity is kept by the electrons traveling from the cathode, on the other hand, positive ion emission from the anode may be neglected for



Distributions in an arc

a) Potential,      b) Current,      c) Space charge

Figure 2-2      Characteristics of Arc Discharges

most arc conditions. It is said that the anode fall is normally of the order of 1-10V (Guile, 1971, Pfender; Young, et. al 1983).

Guile (1971) summarized the common characteristics of the electrode regions, both the cathode-fall region and the anode-fall region, as follows

- (a) High electric and thermal gradients;
- (b) Contraction, i.e. high current densities relative to those of the arc column;
- (c) Plasma jet.

Both electrode regions are the most active areas for polar particles: electrons and ions of gas and those emitted or vaporized from the surfaces of electrodes.

### 2.3 Plasma Devices

A number of reviews have been presented on the different types of plasma-producing devices (Habelrih, Mehmetoglu, Szente, Tsantrizos, etc.). In general we can broadly classify them into two main categories:

#### A. Electrodeless Devices

In this kind of device the energy which is the source of the plasma is transferred from a high frequency ( 1-20 MHz ) electro-magnetic source (for example, a coil ) to the gas by induction. The physical phenomenon governing the operation of the induction plasma is the coupling between the applied high frequency alternating magnetic field and the eddy currents induced in the plasma.(Freeman and Chase, 1968, Munz 1974) The typical configuration of this kind of torch is shown in Figure 2-3.

This technique is most widely used at pressures between a few Torr and one atmosphere. Compared to the other ways of plasma generation the major advantage of this device is to avoid contamination of the plasma system because of the absence of electrodes, allowing the use of aggressive gases, such as chlorine, oxygen and so on.

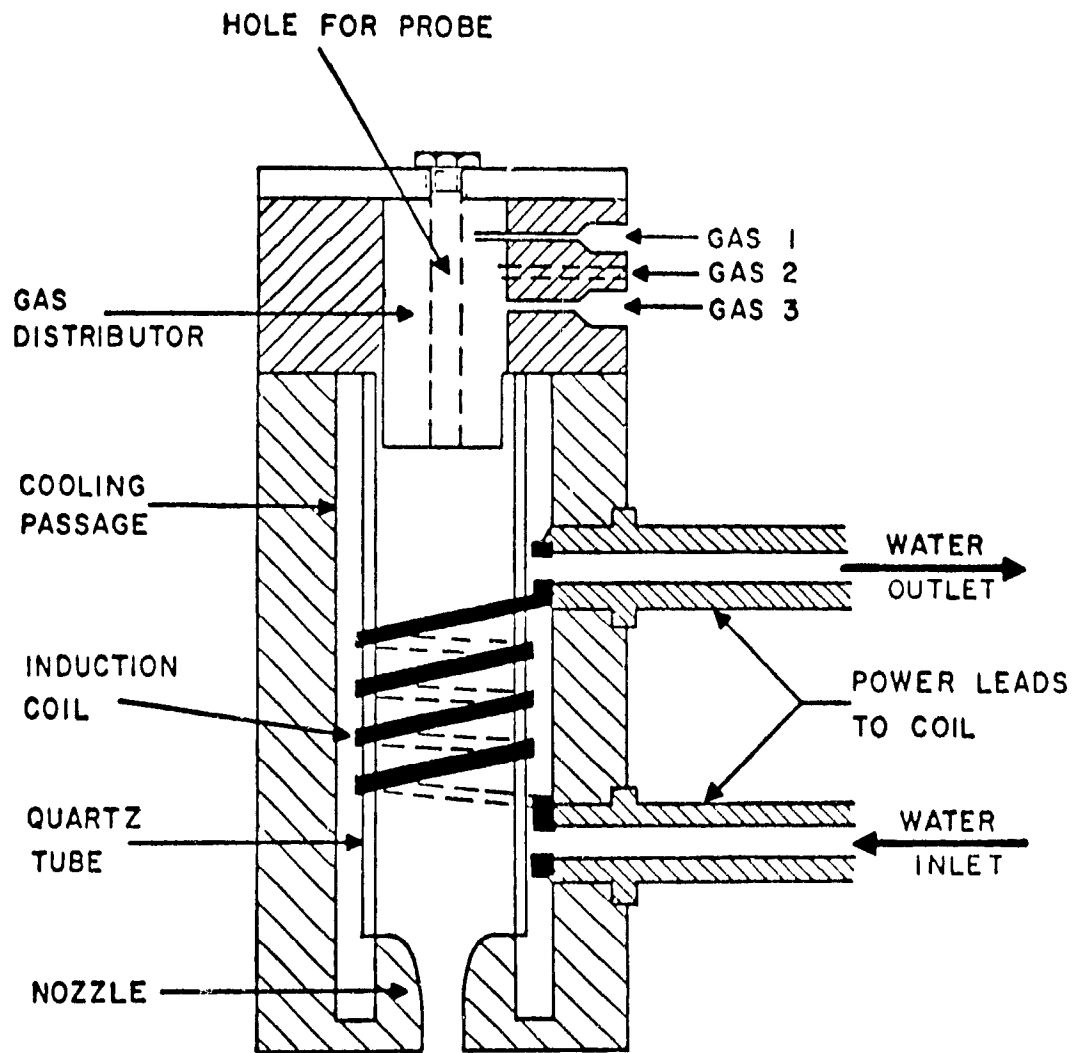


Figure 2-3

Schematic Drawing of RF Plasma Torch

However, for this kind of device, it is not yet possible to transfer more than 40-60% of the electrical energy into the plasma. The minimum power needed for a self-sustained induction discharge is determined by the nature of the gas, the pressure and the frequency of the electromagnetic field. When the frequency is reduced from the MHz range the hundreds of kHz range the minimum power will increase from less than 10 kW to hundreds of kW. To decrease this minimum power the electrical conductivity has to be increased by reducing the pressure or adding ionizing impurities (K, Cs etc.).

The important parameters in the design of an induction plasma torch are:

- Properties of Plasma Gases
- Operating Pressure
- Power Level and Frequency
- Diameter of the Plasma Confinement Tube, and Coil Geometry

It was reported that the RF induction torch was used for treatment of  $\text{TiCl}_4$ ; this will be discussed further in Sec. 4 of this chapter.

## B. Electrode Devices

Just as the name implies, this kind of device always has an anode and a cathode no matter whether the electrodes are fixed or mobile.

### Transferred Plasma Torch

The transferred arc is ignited between two widely separated electrodes in which anode is often a work piece such as a metal to be cut, a pool of molten metal etc. schematically shown in Figure 2-4 (Szente, 1986). The plasma forming gas is injected through the gap between the nozzle and the cathode tip, as a high velocity stream, into the arc column (Sheer, et al, 1969). The energy efficiency of the transferred arc can be made quite high, since the only losses are the cooling of the cathode.

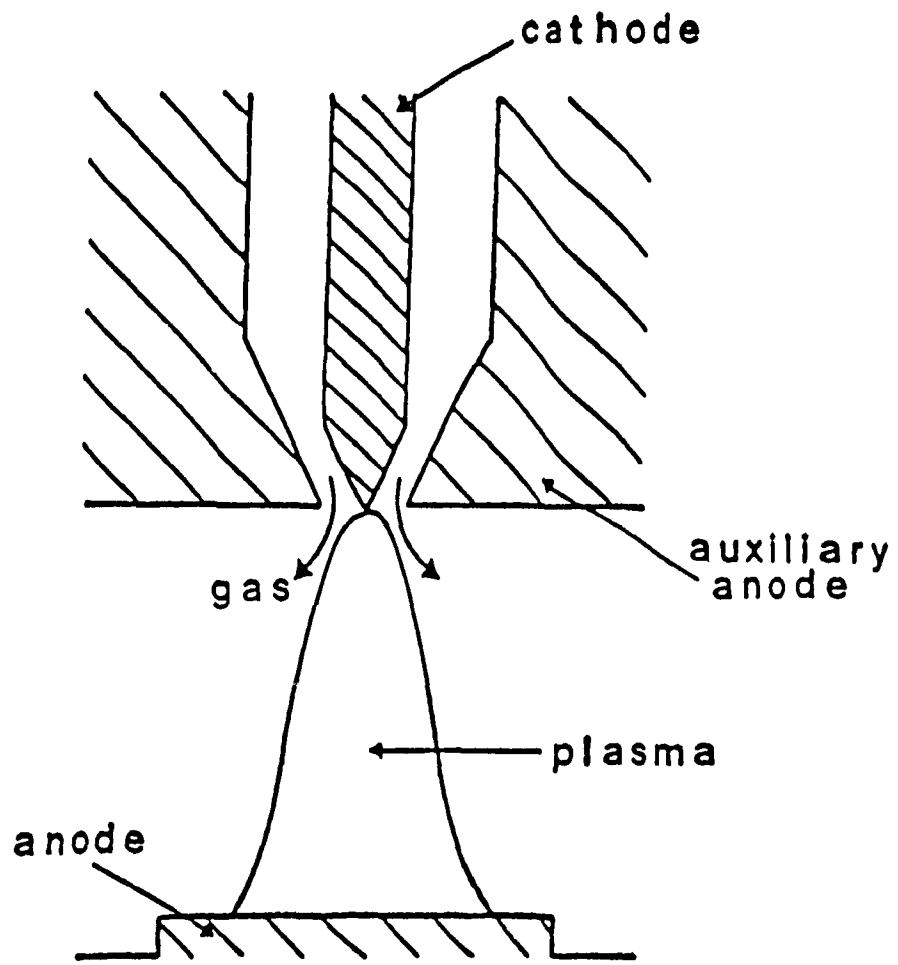


Figure 2-4 Schematic Drawing of Transferred Arc Torch

### DC Plasma Torch

DC-plasma torches are often used as gas heaters and are the type of device used in this research. The DC-plasma torch, powered by direct current, consists of two fixed electrodes, an anode and a cathode. Various torch configurations exist, depending on the arc stabilization modes, which are:

- (a) Tangential gas input in the arc channel;
- (b) Longitudinal gas input along the electrode;
- (c) Segmented Anode arc;
- (d) Magnetic rotation of the arc root, in which the magnetic field can be self induced (by an arc current greater than 800A) or externally generated; the latter was used in our equipment.

Small scale DC plasma torches use a conical tip water-cooled cathode surrounded by an annular water-cooled anode. These may be used at powers up to about 300 kW. For higher power applications torches with two water-cooled co-axial cylindrical electrodes are usually used.

Figure 2-5 (Szente, 1986) shows a typical configuration of a DC Plasma Torch widely used in industry. However the configuration of our DC-equipment (designed by Szente 1986) is different and will be presented in the later chapter.

The energy efficiency of DC plasma torches is higher than that of RF induction torches and may usually be in the range of 65-95%.

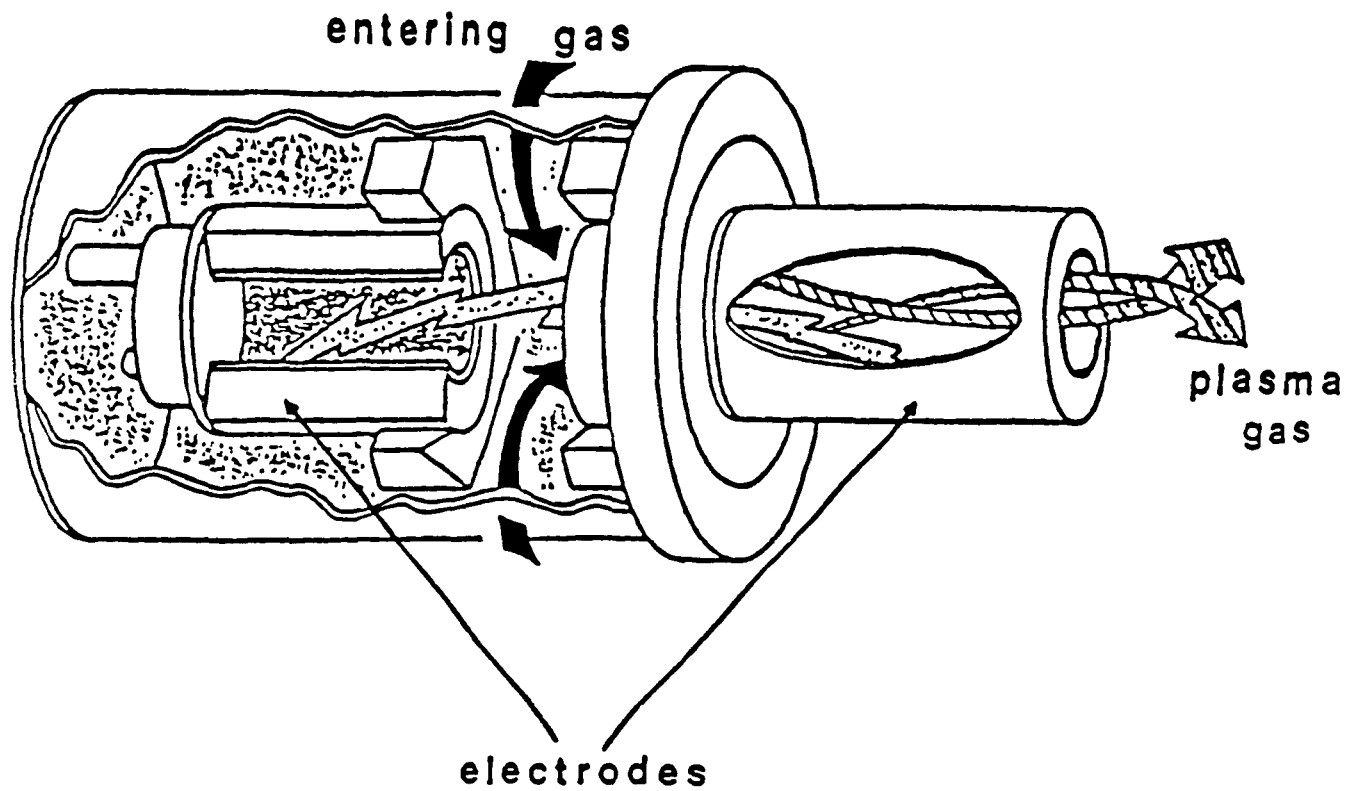


Figure 2-5 Schematic Drawing of the DC Plasma Torch

## 2.4 Phenomena of Electrode Erosion

### A. Introduction

The phenomenon of electrode erosion is a typical feature of plasma electrodes, which may be described by defining the material loss of the electrodes, in grams per Coulomb, as erosion rate of the electrodes. The mechanism of erosion is complicated since it is caused by a combination of melting, evaporating of electrode materials, and chemical reaction between the plasma gas and electrode materials, etc. It was mentioned in general that electrode erosion still limits the lifetime of non-refractory electrodes in plasma arc heater to the order of 200 h for cathodes and less than 1000 h for anodes, and cathodic erosion is more severe and so is more studied (Szente, 1988).

In industrial applications the erosion must be minimized both for economical reasons and for reducing the contamination of the products.

### B. Parameters Affecting Electrode Erosion

From the relative literature and the previous work done by Szente (1986-1989) and Habelrih (1988) it may be summarized that rate of electrode erosion depends on a number of factors, such as:

- i) The Composition of Plasma gases
- ii) Gas Flow Rate
- iii) Arc Current
- iv) Geometry of Electrodes
- v) Materials of Electrodes
- vi) Surface Temperature of Electrodes
- vii) Magnetic Flux
- viii) Arc Velocity

The erosion of copper cathodes in a DC plasma arc heater was studied by Szente (1986) with several gases and by Habelrih (1988) with steam, hydrogen and oxygen. In their research the above factors were separately considered.

As studied in Szente's work the composition of plasma gases may be a sensitive factor in the erosion of electrodes. It was found that small concentrations of any of the polyatomic gases in argon greatly increased the velocity of a magnetically rotated arc and decreased the erosion rate. Four gases, nitrogen, air, ammonia and CO, were tried in his work. No unified relationship was determined, that means: different gases still had their own distinct behavior although similarities existed. Szente showed that addition of these contaminants to argon would also lead to contamination of cathode surfaces in a magnetically rotated arc, and that these surface contaminations changed the arc voltage, velocity and erosion rates by reducing "surface drag", i.e. by changing the ease of electron emission at the cathode surface.

In Habelrih's study, by introducing steam into argon and helium the arc velocity and arc voltage were increased, and the cathode erosion rate was decreased as the concentration of steam in argon increased. This reconfirmed Szente's conclusions.

### C. Improvement of Electrode Erosion

The reduction of erosion of plasma electrodes is always a target of plasma technology development. Improvements can be made in the following areas:

- i) Optimize electrode materials
- ii) Improve design of electrode geometrical configuration
- iii) Increase the efficiency of the cooling system
- iv) Rotate the plasma arc by using magnetic field or aerodynamic means

The latter one is a very successful approach to reducing the erosion rate, because it allows a better distribution of the heat transferred from the arc to the electrode and increases the heat transfer from the arc to the plasma gas. The basic mechanism of

magnetic rotation is that the arc, which is a current conductor, can be rotated by an external magnetic field. The Lorentz force acting on the arc is given by the following expression:

$$F_L = B I d \quad (2-1)$$

where

$F_L$  = Lorentz force

$B$  = External magnetic field strength

$I$  = Arc current

$d$  = Length of the arc in the direction perpendicular to the motion.

The aerodynamic drag force which holds back the arc is:

$$F_d = 0.5 C_d D d \rho V^2 \quad (2-2)$$

where

$C_d$  = Aerodynamic drag coefficient

$D$  = Arc diameter

$\rho$  = Gas density in front of the arc

$V$  = Arc velocity

In addition, if the emission of electrons from the cathode is difficult the arc is also retarded by a surface drag force, denoted  $S$  (Szente, 1986). Therefore, the following general expression can be obtained:

$$F_L + F_d + S = m \frac{dV}{dt} \quad (2-3)$$

where  $m$  is the mass of the particles in plasma arc.

At steady state, the derivative of the velocity on right hand side of the above equation equals zero, that means: the arc velocity is a constant, so that the equation (2-3) can be written as

$$F_L + F_d + S = 0 \quad (2-4)$$

In our project the magnetic force was kept constant, and aerodynamic drag coefficient was assumed constant, which is known as a valid assumption for cylinder in cross flow with Reynolds number between 1000 and 120000 (Perry and Chilton 1973).

## 2.5 Plasma Containing $TiCl_4$

The thermal reduction of  $TiCl_4$  to Ti metal requires that the  $TiCl_4$  molecule is dissociated in a plasma, The cost of Ti metal production was expected to be reduced by a plasma dissociating process and therefore plasmas containing  $TiCl_4$  have been studied since the 1960's.

*By using a RF induction plasma torch*, shown in Figure 2-3, in which the wall of the confinement tube (28-mm i.d.) and inner tube (22-mm o.d.) were made of quartz, with 4-MHz frequency and 10-kW power supply Miller and Ayen investigated the feasibility of reduction of  $TiCl_4$  in 1968. It was reported that  $TiCl_3$  could be produced from  $TiCl_4$  with a very good yield, around 60-90%, by using hydrogen with argon plasma. The temperature was up to 14 000 K and the pressure was one atmosphere. The efficiency of the energy transfer was about 60% or less depending on the features of gas flow and the properties of gases.

However, plasma stability problems limited the  $TiCl_4$  feed rate to a low value so that no more than 1 mole percent of  $TiCl_4$  in argon could be handled in the torch. When  $TiCl_4$  was injected into the plasma tail flame to alleviate stability problems, the quench ring was plugged with deposits and could not be operated for long periods of time.

Early in 1963 Hamish, Heymer and Schallus reported over 60% conversion of  $\text{TiCl}_4$  to  $\text{TiCl}_3$  in the presence of  $\text{H}_2$  in a high temperature arc torch, but the details of the torch were not given.

By using a transferred-arc torch, shown in Figure 2-4, Tsantrizos reported that a stable transferred arc was produced with gases containing up to 20 mole percent of  $\text{TiCl}_4$  in argon, helium and argon-helium mixture. When aluminium was used as reductant about 60% of all titanium fed into the reactor was collected, and the related erosion results of cathodes are shown in Table 2-1. In his experiments tantalum carbide was used for the cathode tip instead of the commonly used thoriated tungsten cathode tip. Tsantrizos showed that a thoriated tungsten cathode would not provide stable operation, resulting in the increasing voltage fluctuation, shown in Figure 2-6. A thoriated tantalum carbide cathode resulted in stable operation and small voltage variations, shown in Figure 2-7. All plasmas were operated by using identical conditions of 10-15 L/min main plasma gases with 6-25 g/min of  $\text{TiCl}_4$  gas at 200 A arc current.

From the 1960's to the 1980's some other workers, such as Akashi, et. al (1977) Atamonov, et. al (1978) and Kikukawa, et. al (1983) investigated the possibility of forming Ti metal from a mixture of  $\text{TiCl}_4$  and hydrogen introduced into the tail flame of a DC argon plasma torch. They did not feed the chloride into the current transferring region between cathode and anode. The electrode materials were not reported. Even so the concentrations of  $\text{TiCl}_4$  were extremely low and it was reported that stability of the arc was a major problem.

Table 2-1 Experimental Data on Cathode Erosion

PlasmaGas (L/min)	ArcLength (cm)	TiCl <sub>4</sub> Feed (g/min)	ArcVoltage (V)	ErosionRate (mg/min)
10 - Ar	2.0	0.0	26	0.0
10 - He	1.3	0.0	34	0.0
10 - H <sub>2</sub>	2.0	0.0	77	0.1
10 - H <sub>2</sub>	2.0	20	72	120
5 - Ar + 5 - H <sub>2</sub>	2.0	1.0	55	3.5
15 - Ar + 15 - H <sub>2</sub>	2.0	5.0	67	13
5 - Ar + 5 - H <sub>2</sub>	2.0	5.0	62	170
10 - Ar	1.3	12.5	54	210

Ref. Tsantrizos, 1988

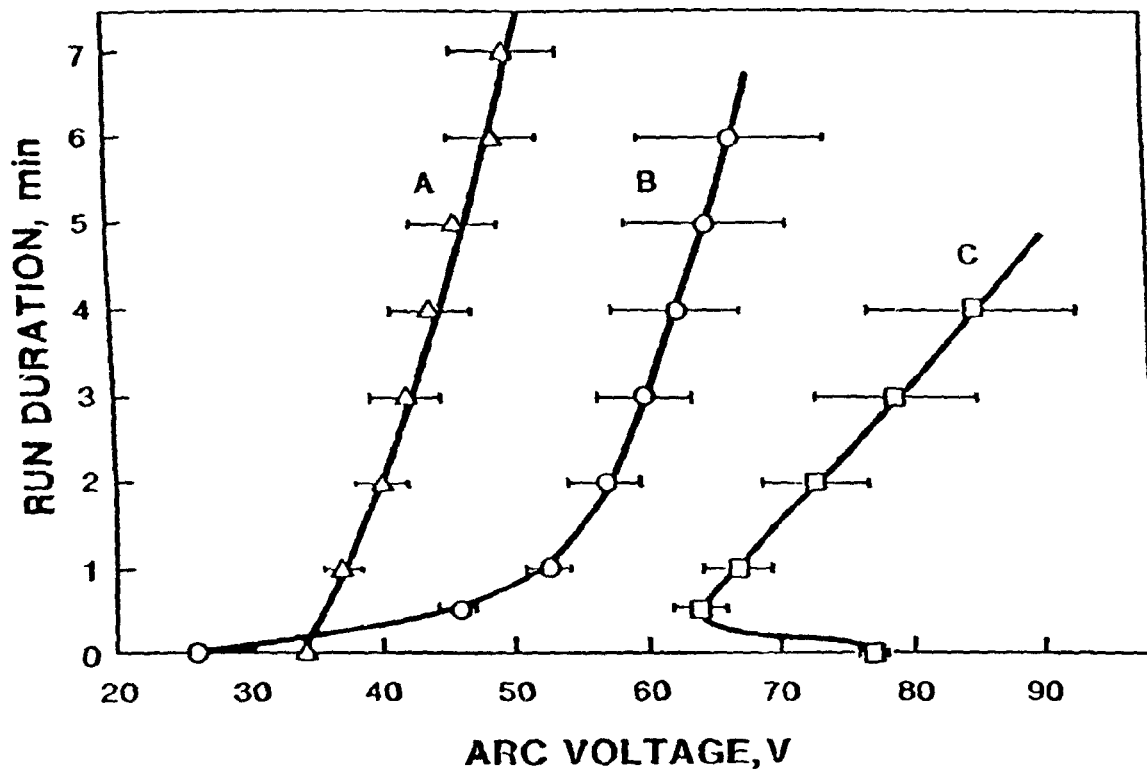


Figure 2-6

Arc Voltage Variations with Time for  $\text{TiCl}_4$ -Rich  
Arcs Using a Thoriated Tungsten Cathode

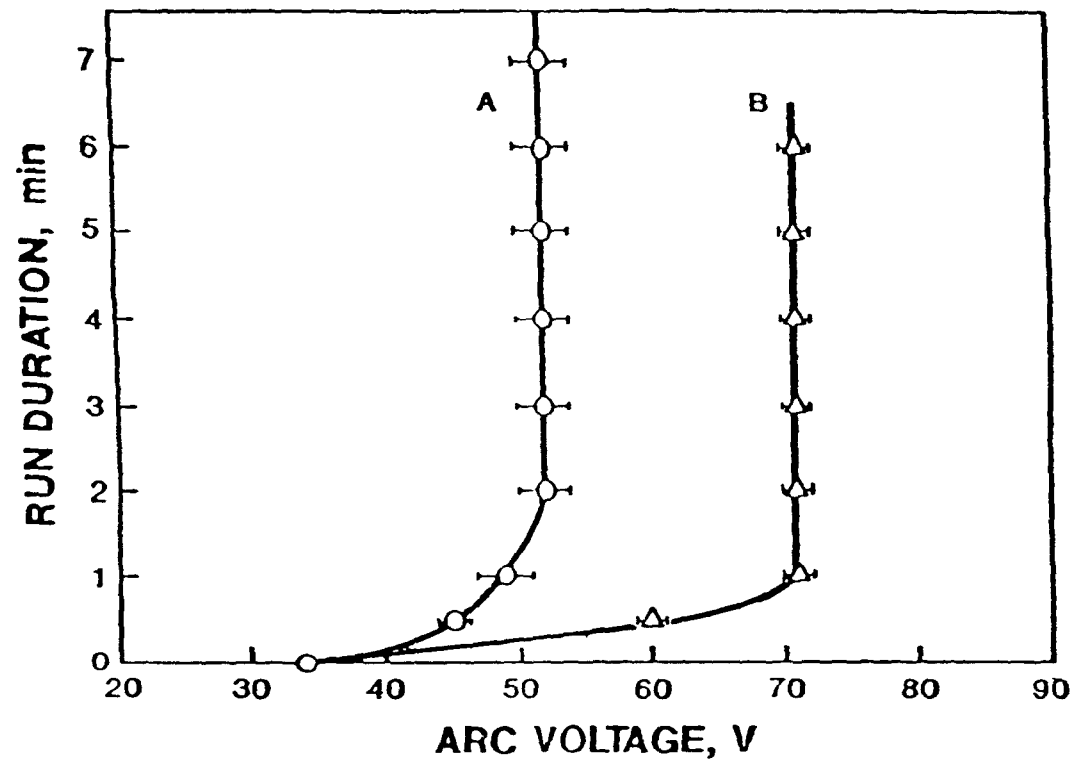


Figure 2-7 Arc Voltage Variations with Time for  $\text{TiCl}_4$ -Rich Arcs Using a Thoriated Tantalum Carbide Cathode

## **CHAPTER 3.**

### **EXPERIMENTAL APPARATUS**

---

#### **3.1 Introduction**

The equipment that was used in the experiments consists of the following main components:

- i. The DC-Plasma Torch (test chamber & electrodes);
- ii. The Plasma Gas Feeding System;
- iii. The Exhaust Gas Treatment System
- iv. The Heating/Cooling System
- v. The Data Recording System;
- vi. The Power Supply

Figure 3-1 is a schematic drawing of the overall experimental set-up.

#### **3.2 The DC-Plasma Arc Torch**

The reactor assembly, shown in Figure 3-2, is a modified version based on the Habelrih's reactor (1988) which was based on the original design of Szente (1986). The main characteristics of this reactor, such as dimension (internal diameter and height of the chamber are 9.8 cm and 30 cm, respectively) and the design of coil (average DIA is about 34 cm and height is 23 cm with 210 turns. The copper tubing covered with electrical tape and the coil layers separated by 0.25 mm thick mylar sheet for electrical insulation) of the reactor were not changed, and were described in the thesis of Habelrih (1990). The main modifications made in this study include the following:

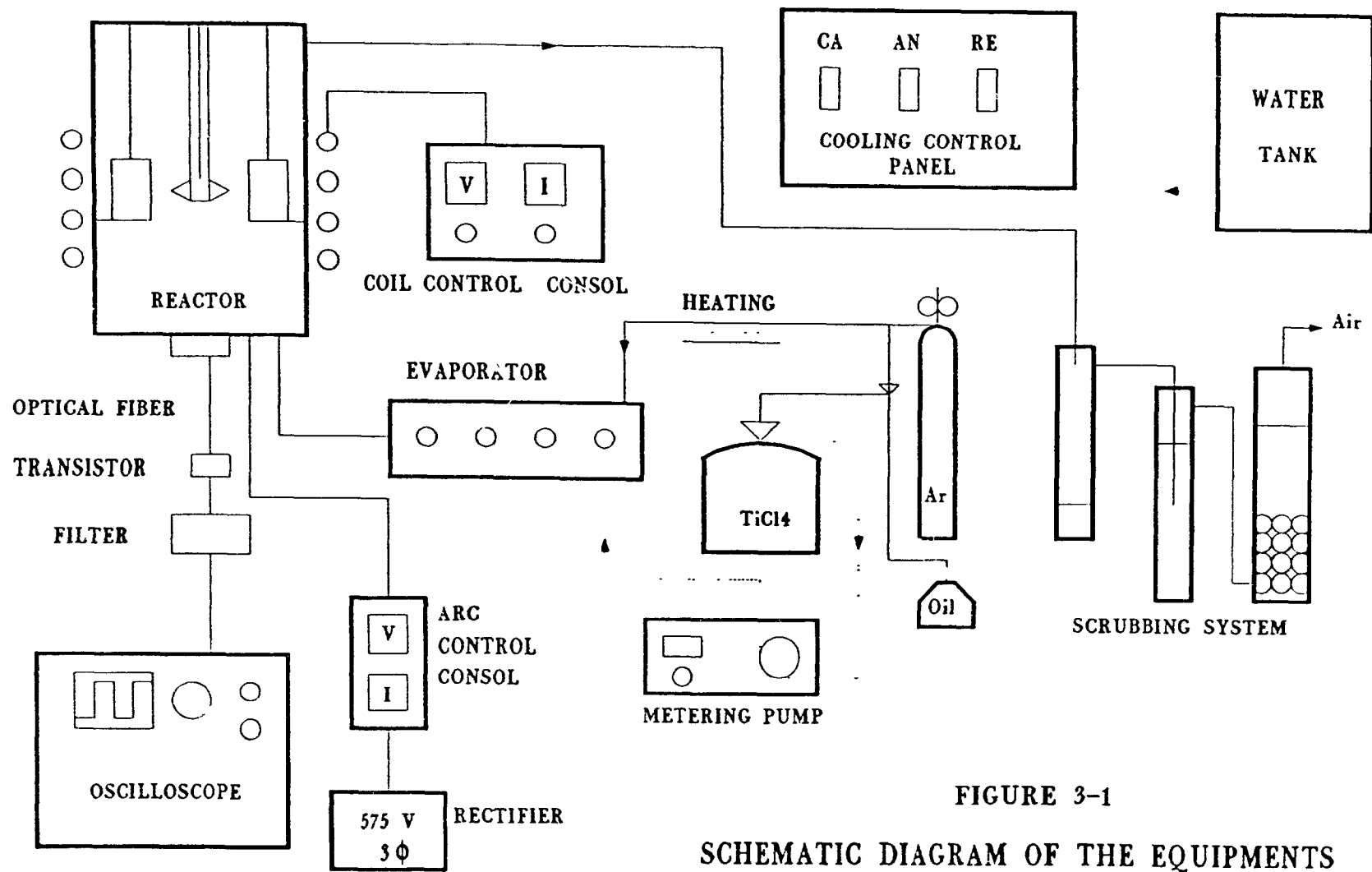


FIGURE 3-1  
SCHEMATIC DIAGRAM OF THE EQUIPMENTS

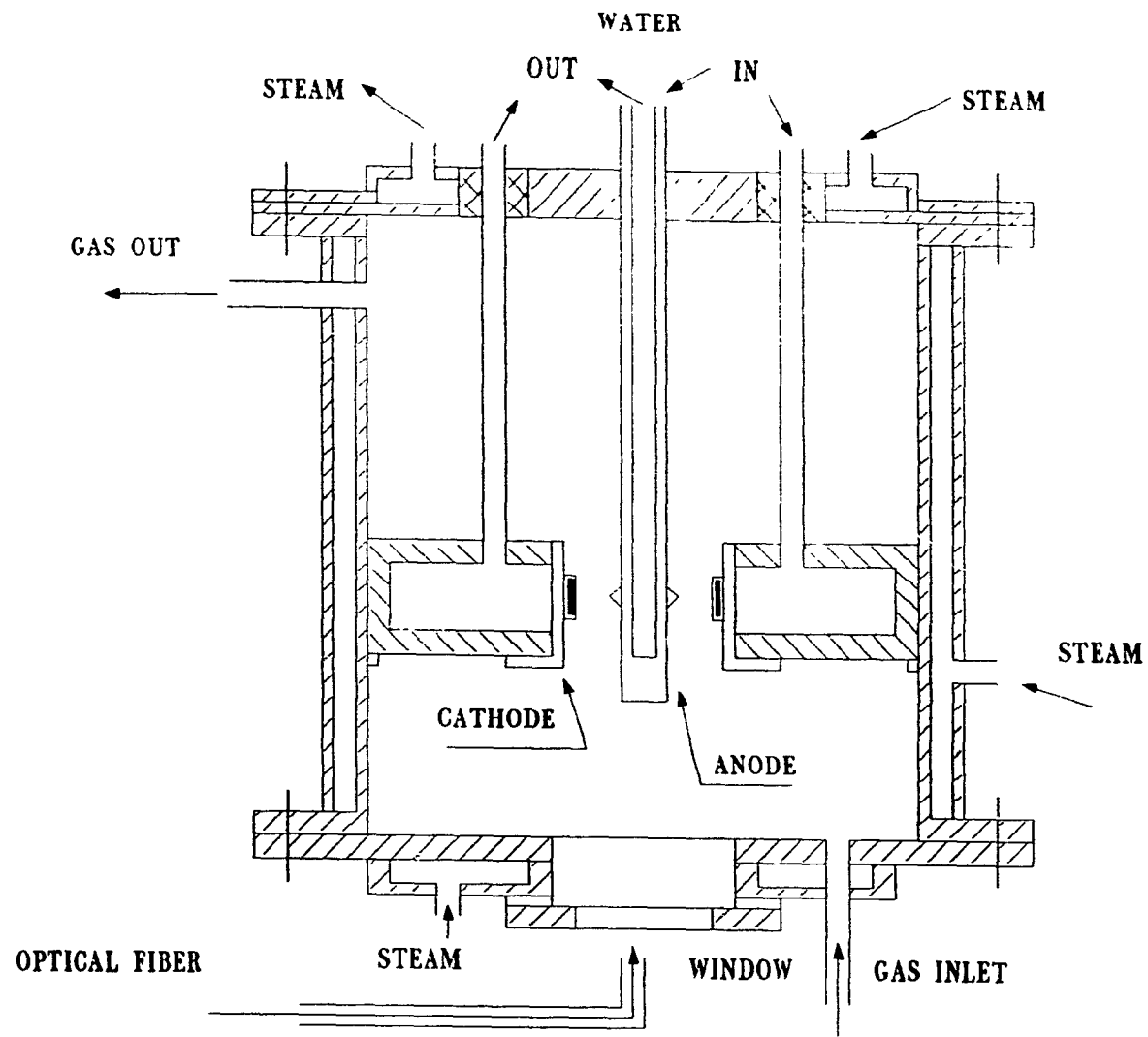


FIGURE 3-2 SCHEMATIC DRAWING OF THE REACTOR ASSEMBLY

### A. The Configuration of the Electrodes

The cooling tubing of the anode was designed as a dual tube construction (in and out at the one side of the reactor) in which the internal thinner tubing, made of brass, is the inlet line and the space between two tubing walls (outside tubing made of stainless steel #316, 9.53 mm OD, 1.14 mm wall thickness, and 43.2 cm long) is the outlet path. The inside tube was well centered and fixed to avoid nonuniform flow and vibration of inner tubing, which would decrease the efficiency of the cooling.

The anode tips were made of Cu, TaC+Al or Ta. The Cu tips were directly machined on the tubing, the other tips were machined to be small pointed rings mounted on the tubing, as shown in Figure 3-3. The external diameter and the height of the tip were about 20.1 mm and 10.2 mm, respectively.

The cathodes were made of TaC and TaC+Al, respectively, as a cylindrical ring mounted in a copper holder, shown in Figure 3-3. The internal diameter of the ring was 24.1 mm and the height was about 10.2 mm.

The purpose of this change was to fit a viewing window at the center of the bottom of the reactor, through which the behavior of the arc could be clearly observed, and also to ease the installation of the anode tip.

### B. The Extension of the Reactor

In previous experiments done by Szente and Habelrih, the gases were not strongly corrosive. The exhaust lines were made of rubber and plastic tubes which were not acceptable for the extremely corrosive and toxic titanium tetrachloride. The whole exhaust system was modified for this work. Only stainless steel #316 proved to be suitable for the gas at high temperature. In order to simplify the arrangement of the lines for rapid replacement of the test electrodes and for safe operation the four exhaust lines on the top flange of the reactor were changed to a single 9.53 mm OD side line which is mounted on the extension of the reactor, shown in Figure 3-2.

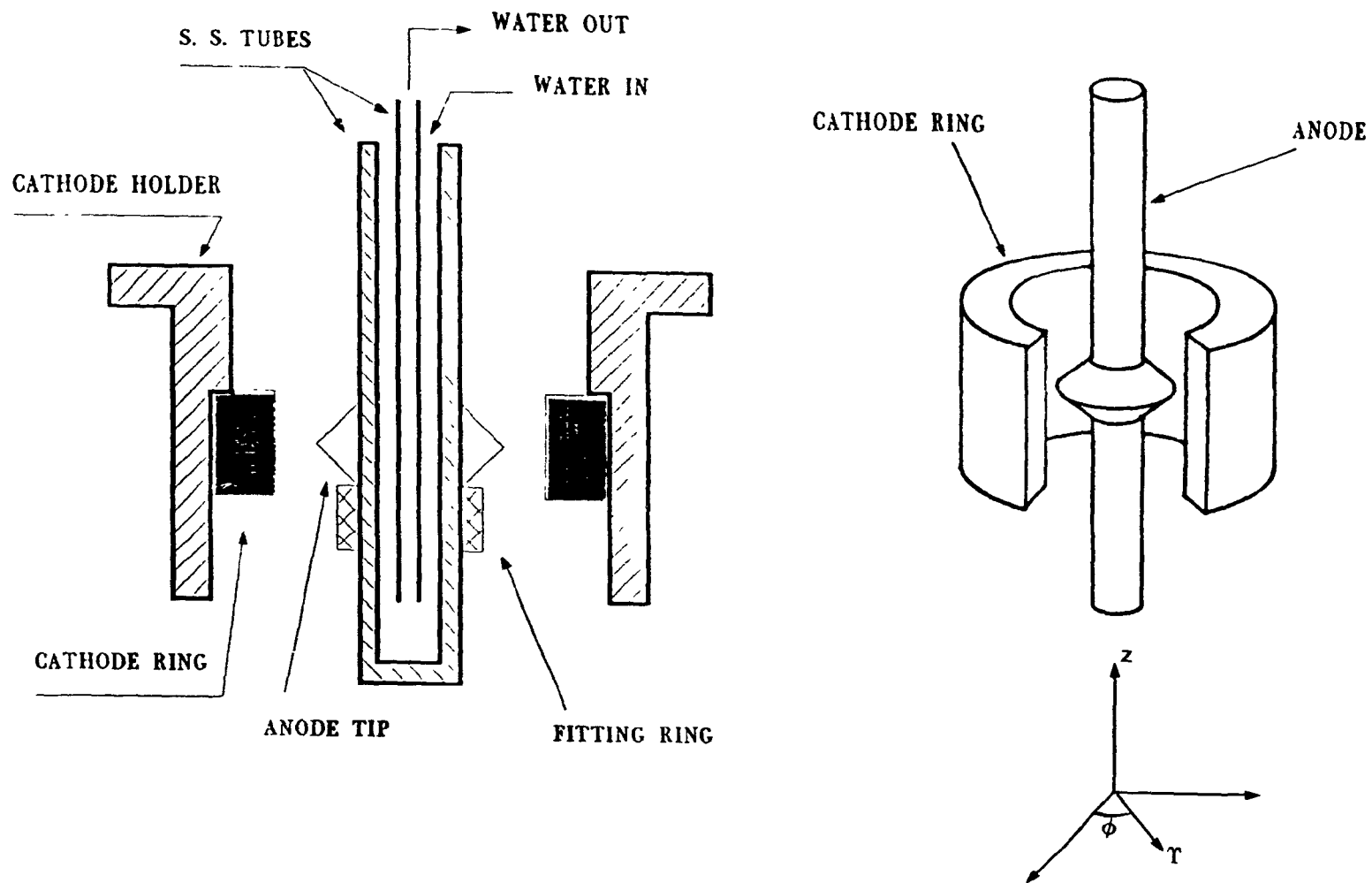


FIGURE 3-3 SCHEMATIC DRAWING OF THE ANODE AND CATHODE

### C. The Viewing Window

The window on the bottom of the chamber was made of a 6.35 cm diameter and 6.35 mm thick quartz glass which is O-ring sealed to prevent leakage of the gas, and attached with a screw ring to the lower flange for visual observations of the arc

### D. The Relocation of the Optical Fiber

In order to measure the velocity of the arc an optical fiber was introduced in a stainless tube into the chamber in both Szente's and Habelrh's reactors. The light of the arc passed through the fiber out of the reactor and was transformed by a transducer into an electrical signal which can be shown on an oscilloscope. Because of the very high operating temperature and corrosive gas in the new experiments, the internal installation of the optical fiber was not longer suitable, The big window made it possible to mount the optical fiber outside of the reactor close to the window.

### E. Plasma Gas Feed Lines

In order to feed the high temperature and corrosive plasma gases, the gas inlet line was made of stainless steel which was arranged on one side on the bottom flange. This line was trace heated by using four heating tapes rated at 500 W each.

## 3.3 The Feeding System

The feeding system consists of a cylinder of liquid titanium tetrachloride provided by Akzo Chemicals Ltd, a metering pump ( model P10T) made by Fred A Dungey Inc., and an evaporator heated with five cartridge heaters (240V, 500W/each) which is used for vaporizing the liquid of titanium tetrachloride into argon gas

All fixed gas feeding lines were made of #316 stainless steel, 6.35 mm OD, 0.99 mm wall, and heated by using heating tapes far above the boiling point, 406 K, of the  $\text{TiCl}_4$  liquid to avoid the condensation of the gas. Actually in our experiments the gas was greatly superheated: the temperature of the evaporator was heated up to 623-773 K and the the temperature of the lines was elevated to 453-473 K. A pressure relief line and a unit (a bubbler) filled with silicone oil were arranged to maintain the pressure in the  $\text{TiCl}_4$  cylinder slightly higher than one atmosphere. The arrangement of the  $\text{TiCl}_4$  feeding system is shown in Figure 3-4.

### 3.4 The Scrubbing System

The scrubbing system was designed to clean the gases leaving the reactor before venting them to the atmosphere. These gases contain various toxic and corrosive chemicals, such as subchlorides, chlorine gas, and possibly oxychlorides.

The scrubbing system consists of two plastic bottles (4 L each) and a plastic tower (10.2 cm ID x 122 cm high, volume 9 L), all of which contained 5-10% sodium hydroxide (NaOH) solution.

i. The first bottle contained only 0.8 L of NaOH solution so that the solution could not be sucked into the test chamber in the event of negative pressure caused by the extinction of the arc. Two bulkhead unions mounted on the top of the bottle served as the gas inlet and exhaust.

ii. The second bottle was similar to the first one but was filled with 3 L of the NaOH solution, and contained an inlet tube to lead the gases below the scrubbing solution surface.

iii. The tower contained 4.5 L of NaOH solution and about two hundred 13 mm diameter spherical plastic packing to ensure good gas-liquid contacting.

The basic features of the scrubbing system are given in Figure 3-5.

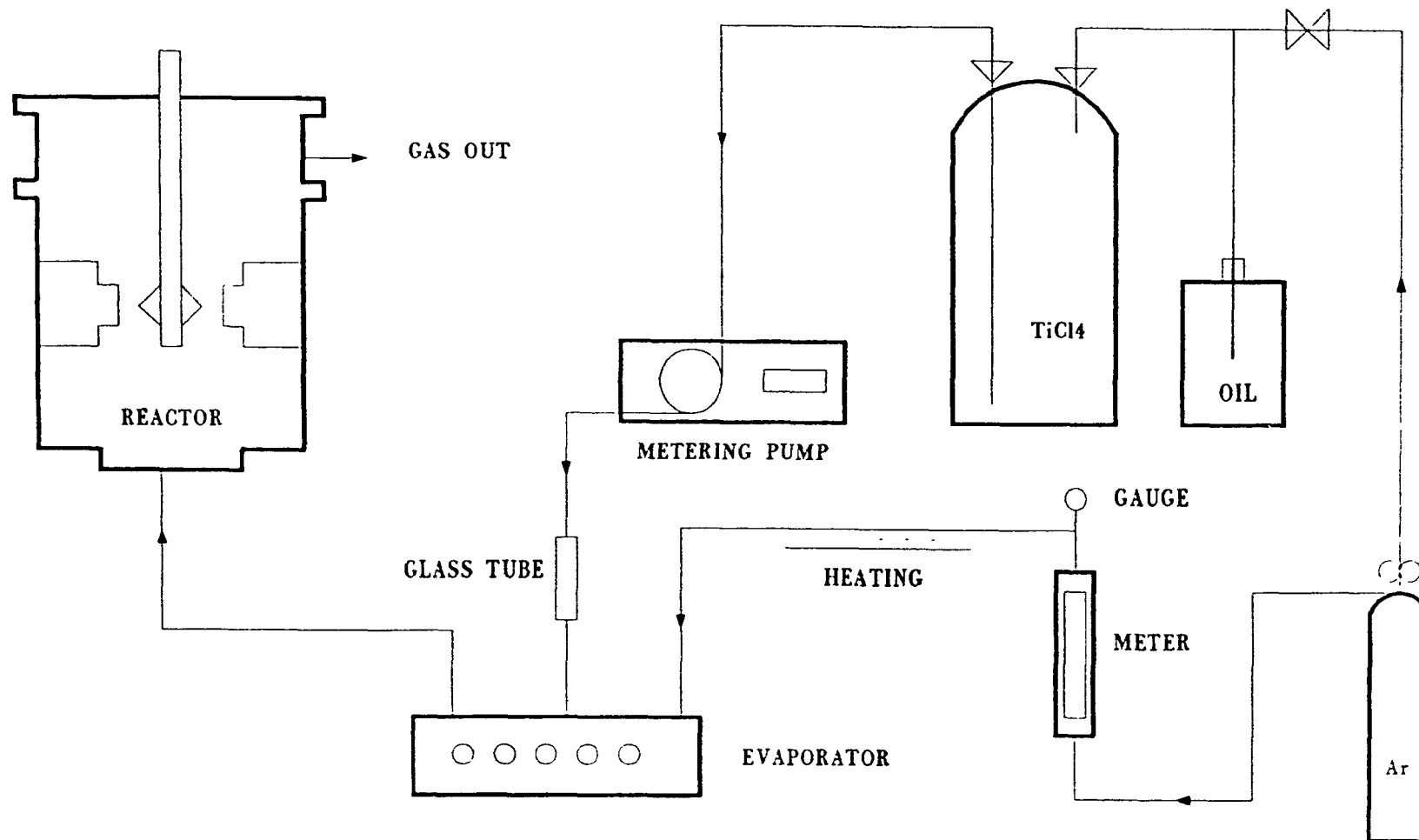


FIGURE 3-4 SCHEMATIC DRAWING OF FEEDING SYSTEM

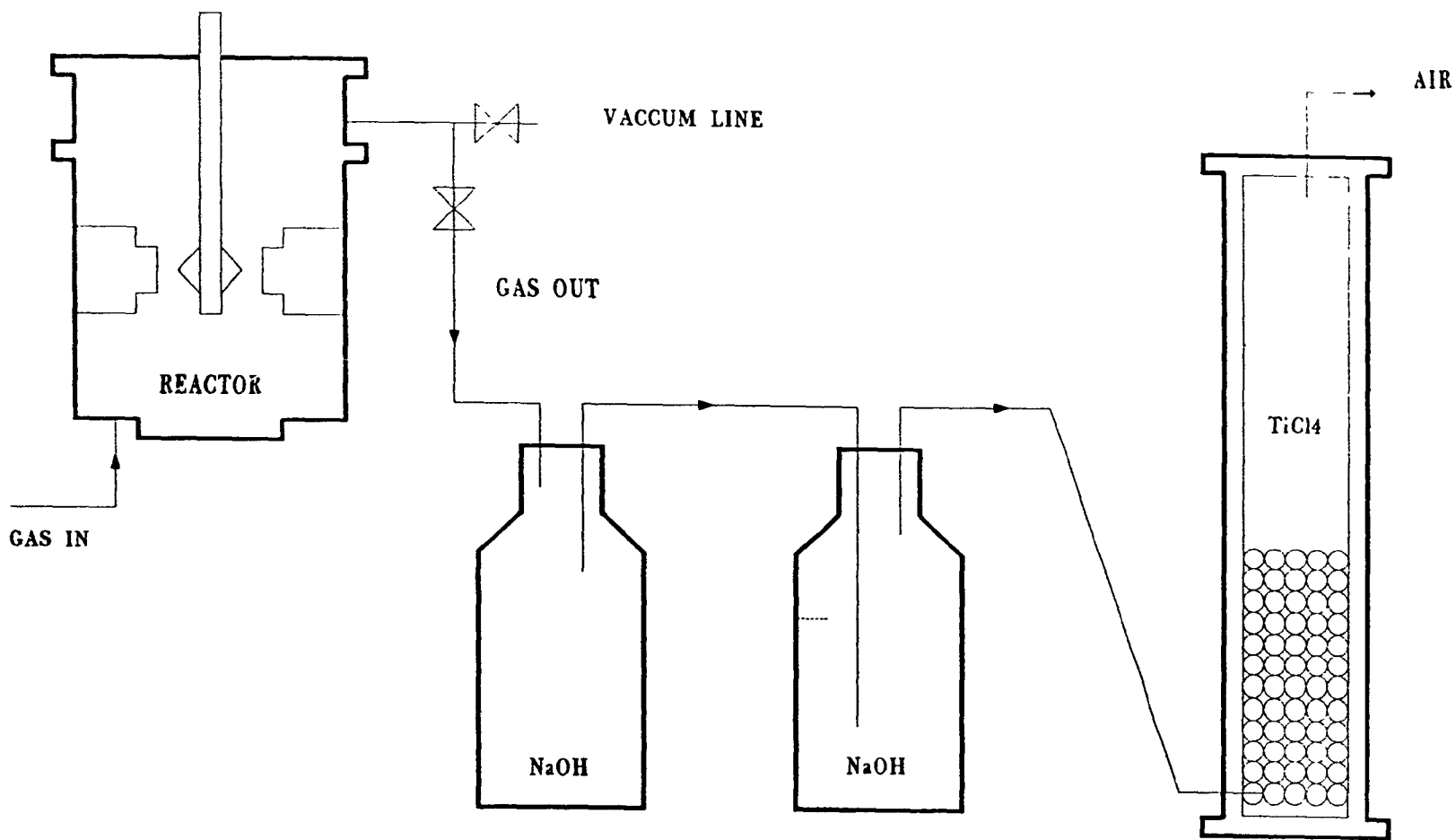


FIGURE 3-5 SCHEMATIC DRAWING OF SCRUBBING SYSTEM

### 3.5 The Heating/Cooling System

The cooling system is similar to that used by Habelrih. This was originally a triethylene glycol loop system containing a 115 liter stirred tank heated up with a 6 kW immersion heater to a maximum temperature 393 K which is thermostatically controlled, and a manually controlled water cooling coil (Habelrih 1990).

The modification of the system was based on the consideration that the condensation of  $\text{TiCl}_4$  (409 K) should be avoided so that the concentration of  $\text{TiCl}_4$  in the plasma gas was precisely known. The cooling efficiency of triethylene glycol is not as good as that of water and, in addition, it is difficult to clean the glycol from the reactor and the electrode surface. It was finally decided to cool both electrodes with hot water at about 363 K, and to heat up the reactor wall and flanges with steam at around 375 K.

### 3.6 The Data Recording System

The system includes the following equipment:

- i. Two flow meters for the cooling water of anode and cathode;
- ii. One rotameter for argon gas and a metering pump for controlling of the flow rate of  $\text{TiCl}_4$  liquid;
- iii. A set of thermocouples for measuring temperatures of the cooling water, steam and gases;
- iv. Two pressure gauges for measuring the pressures of inlet and outlet gas lines;
- v. An oscilloscope for observing the behavior of the arc and measuring the velocity of the arc;
- vi. A strip chart recorder for recording the voltage of the arc;

- vii. Two ammeters for monitoring the currents of the arc and the coil;
- viii. Two voltmeters for monitoring the voltage of the arc and coil.

### **3.7 Power Supplies**

The power was provided to the arc either by a Thermal Dynamics rectifier model (TDC 1A40) with a maximum power of 45 kW and a 320 V open circuit voltage or by an assembly of four Miller (SRH-444) rectifiers connected in series with a total open circuit voltage of 305 V and a maximum power output of 78.4 kW. The coil was powered by a Syntron rectifier model (P0063) with a maximum output voltage of 40 volts. A control console was used to measure and adjust the current to the arc. The voltage of the arc was plotted on the strip chart recorder with a full scale accuracy of 2.5V.

### **3.8 The High Frequency Unit**

A Miller (HF 250-1) unit with a frequency of 10 kHz was connected in series with the DC power supply to initiate the breakdown of the arc gap.

## **CHAPTER 4.**

### **EXPERIMENTAL PROCEDURE**

---

#### **4.1 Introduction**

The experimental procedure used in this study contains three parts summarized as follows:

1. Preparation before tests
2. Operating during tests
3. Treatment after tests

#### **4.2 Preparation of Experiments**

##### **A. Preparation of Electrodes**

The electrodes are the critical parts in our experiments, and the following procedure was set up for their use.

1. The electrodes, the cathode holder, and the anode tubing were cleaned with dry tissue paper and pressurized air;
2. The sizes of both the cathode ring and the anode tip were measured, especially the inside diameter of the cathode ring and outside diameters of the anode tip to ensure the correct interelectrode spacing;
3. The cathode ring and anode tip were weighed. The purpose of this step was to get data of erosion rate of electrodes;
4. The cathode ring and the anode tip were mounted onto the cathode holder and the anode tube, respectively. Electrodes should be mounted tightly to ensure as good an electrical contact as possible;

5. The two electrode assemblies were weighed again for reference;
6. A thin layer of ceramic was pasted onto the inside surface of the cathode holder and the outside surface of anode tubing to ensure that the arc strikes only the anode tip and the cathode ring;
7. The ceramic pastes were dried in an oven at 100 °C for two hours.

#### B. Cleaning Procedure of the System

Because the  $\text{TiCl}_4$  gas is very corrosive the cleaning procedure was followed:

1. The inside of the reactor chamber were thoroughly cleaned and dried to remove residual powder of products from the last test;
2. All feeding and scrubbing lines were cleaned and dried;
3. The evaporator and the scrubbing bottles and tower were cleaned and dried.

#### C. Assembly Procedure

1. The anode and the cathode holder were mounted into the reactor. The anode tip was well centered;
2. All "O" ring seals were properly checked to ensure they are in good condition;
3. The reactor chamber was securely closed to avoid leakage;
4. All lines were connected( feeding, scrubbing, cooling and electrical cables ).

#### D. Pre-Check Procedure

It was ensured that the following units are in good condition:

1. The main working gas supply ( the cylinder, valves and gauges );
2. The  $\text{TiCl}_4$  feeding system ( the metering pump, valves and the cylinder);

3. The evaporator and heating system ( thermocouples, heating rods, heating tapes, the thermal meter and steam heating of chamber wall );
4. The electrical power supply ( the rectifier units, connections, the control panel and meters );
5. The magnetic coil ( switch, connection and meters);
6. The cooling system ( the water tank, the immersion heater, meters, connections ).

### 4.3 Operation of Experiments

#### A. Starting Procedure

1. The heating system, including the evaporator, the gas line heating tapes and the immersion heater for water was switched on;
2. The system was evacuated to - 100 kPaG and then purged with argon gas;
3. The cooling water supply for the reactor chamber and the magnetic coil was started;
4. Steam was fed to heat the wall of the reactor up to about 375 K;
5. The voltage to the coil was adjusted to 38 V;
6. The argon flow was adjusted to 15 L/min;
7. The  $\text{TiCl}_4$  liquid was prepumped about two minutes to fill the tube leading to the evaporator. The pump was stopped just before the liquid reached the evaporator so that  $\text{TiCl}_4$  was available immediately after starting the arc with argon.

#### B. Operating of Tests

1. The arc was ignited with the high frequency unit;
2. The current was adjusted to the desired value;

3. The  $\text{TiCl}_4$  liquid was fed according to the preset flow rate;
4. The strip chart recorder and the oscilloscope were turned on;
5. Any change in the pressure in the chamber was closely observed;
6. The following data were measured:

Voltage of the arc;

Velocity of the arc;

Flow rate of argon gas and  $\text{TiCl}_4$  liquid, and cooling water;

Temperature of gases, and inlet & outlet cooling water;

Time of the running.

#### 4.4 Post-Treatments

1. The whole system was purged with argon gas until the exhaust gas appeared clear;
2. The reactor chamber was opened and the electrode assembly removed;
3. The electrodes were cleaned with water;
4. The cathode ring and the anode tip were disassembled for weighing;
5. A sample of solid reaction product was collected from the chamber and sealed it in a plastic bag immediately;
6. The system was cleaned.

## CHAPTER 5.

### PIONEERING ANALYSIS

---

#### 5.1 Thermodynamic Considerations

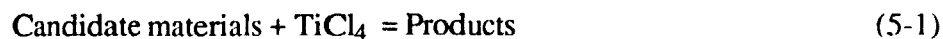
##### A. Basic Thermodynamic Calculations

The purpose of this study was to identify some suitable electrode materials which have negligible chemical reaction with titanium tetrachloride plasma gas. A thermodynamic analysis of candidate materials was therefore conducted.

The calculations were carried out on the mainframe computer system of McGill University by using the F\*A\*C\*T - Thermodynamics Analysis Program which is a package of softwares including the REACTION and EQUILIBRIUM programs used in our calculation.

The first screening was to examine the free energy of reactions of materials with a high melting point and acceptable electrical conductivity, with  $\text{TiCl}_4$  to form chlorides by using the REACTION program. This program computes the changes in thermodynamic state functions of a balanced chemical reaction, and is much less expensive than the EQUILIBRIUM program.

Generally, chemical reactions to be considered can be expressed as

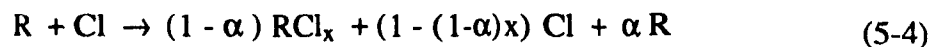
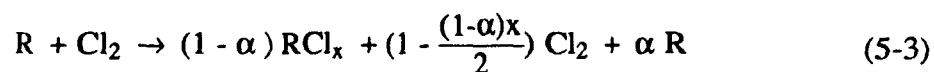


for all candidate materials, the Gibbs Free Energy changes were calculated at 2000 K and a pressure of one atmosphere. If the free energy of the reaction is much greater than 0 it is reasonable to predict that the reaction will not occur spontaneously, meaning the candidate material might be inert to  $\text{TiCl}_4$ . However, it should be noted that the

molecules of  $\text{Cl}_2$  and the atoms of Cl would exist in the  $\text{TiCl}_4$  plasma gas due to dissociation and ionization of  $\text{TiCl}_4$ ; these were also considered as reactants. Table 5-1 is a summary of the most successful results.

The overall calculations of chemical reaction, based on the Data-Base of the mainframe computer system, covered most high melting compounds of oxygen, chlorine, carbon, boron, and nitrogen, with elements of Group IIIB, IVB, VB, VIB, VIIB, and VIII.

Following this inexpensive initial analysis, the EQUILIBRIUM program was used to calculate the extent of reaction of the most successful candidates with  $\text{TiCl}_4$ ,  $\text{Cl}_2$  and Cl according to the reactions given below



This program uses free energy minimization to determine all possible reaction products for a specific reactant stoichiometry, T, and P. The results are summarized in Table 5-2. The values of the table must be treated with caution since they are based on equilibrium and do not take into account the kinetics of the various reactions. The true situation is bound to be one of non-equilibrium because there are enormous thermal gradients between the plasma and the electrode. The three values of  $(1-\alpha)$  given in Table 5-2 show the effect of changing reaction stoichiometry. The first column includes titanium and four chlorine atoms, the second two chlorine atoms and the last only one chlorine atom.

**Table 5-1. The Results of Chemical Reaction Analysis**

Material Name	Formula	Melting T K	------(2000 K)-----		
			TiCl <sub>4</sub>	Cl <sub>2</sub>	Cl
Tantalum Carbide	TaC	4152	N	Y	Y
Scandium Oxide	Sc <sub>2</sub> O <sub>3</sub>	2500	N	N	N
Tantalum Diboride	TaB <sub>2</sub>	3373	N	N	N
Aluminium 12-Boride	AlB <sub>12</sub>	3373	N	N	N
Silicon Carbide	SiC	3200	N	N	N
Ditungsten Carbide	W <sub>2</sub> C	3068	N	N	N

Note: "N" means  $dG \gg 0$  ( $> 100$  kJ), no spontaneous reaction, and  
 "Y" means  $dG \ll 0$  ( $< -100$  kJ), reaction could occur.

**Table 5-2. The Results of Equilibrium Analysis at 2000 K**

Material Name	Formula	Melting T. K	TiCl <sub>4</sub>	Cl <sub>2</sub>	Cl
			(1- $\alpha$ )	(1- $\alpha$ )	(1- $\alpha$ )
Tantalum Carbide	TaC	4152	0.00	0.50	0.25
Scandium Oxide	Sc <sub>2</sub> O <sub>3</sub>	2500	0.00	0.00	0.00
Tantalum Diboride	TaB <sub>2</sub>	3373	0.00	0.20	0.10
Aluminium 12-Boride	AlB <sub>12</sub>	3373	0.26	0.052	0.026
Silicon Carbide	SiC	3200	0.33	0.67	-----
Ditungsten Carbide	W <sub>2</sub> C	3068	0.00	0.5	0.25

Note: The values of 1- $\alpha$  in the Table indicates the reactivities of the materials

## B. Conclusion

From the above analysis it is known that in thermodynamic sense, even though the temperature in the calculations is only up to 2000 K and, while the temperature of a plasma arc will be much higher, we may predict that the following materials could be successful electrodes used in  $\text{TiCl}_4$  plasma gas:

- i. TaC Tantalum Carbide
- ii.  $\text{TaB}_2$  Tantalum Diboride
- iii.  $\text{Sc}_2\text{O}_3$  Scandium Oxide
- iv.  $\text{W}_2\text{C}$  Tungsten Carbide

However due to the limitations of time and budget only the TaC was used in our experiments.

## 5.2 Preliminary Experiments

### A. Preparation of Pure TaC Cathode Rings

The TaC cathode rings, schematically shown in Figure 3-3, were prepared by Dr. K. Shanker of the Department of Mining and Metallurgical Engineering, McGill University, from TaC powder made by Hermann C. Starck Berlin. The composition of the powder is shown in Table 5-3 and the basic process flow chart of making the cathode ring is presented in Figure 5-1. The rings in different stages (from powder to a machined ring in four stages) are shown in Figure 5-2. Through the analysis of the SEM it is found that the microstructure of the cathode ring is porous, as shown in Figure 5-3; depending on the time of sintering the density of the rings is in the range of 40-80% of the theoretical value.

**Table 5-3      The Composition of TaC powder**

<b>Contents</b>	<b>Concentration (%)</b>
C total	6.18
C free	0.05
Ca	0.001
Fe	0.003
Nb	0.10
Si	0.001
Ti	0.001

Source:            Hermann C. Starck Berlin    GmbH +Co. KG (23 Feb., 1990)

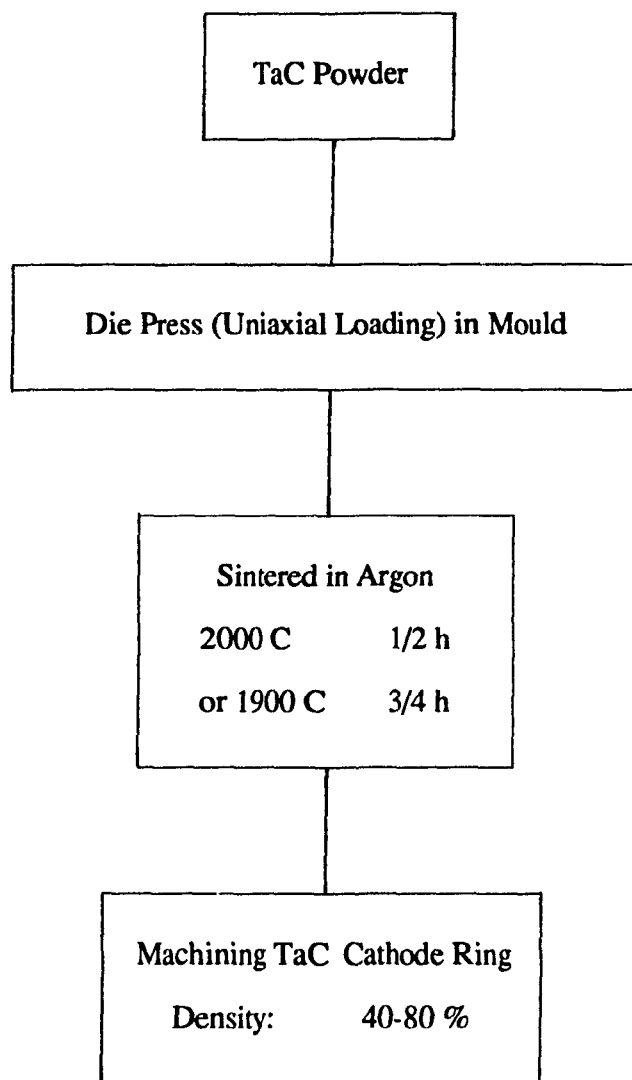
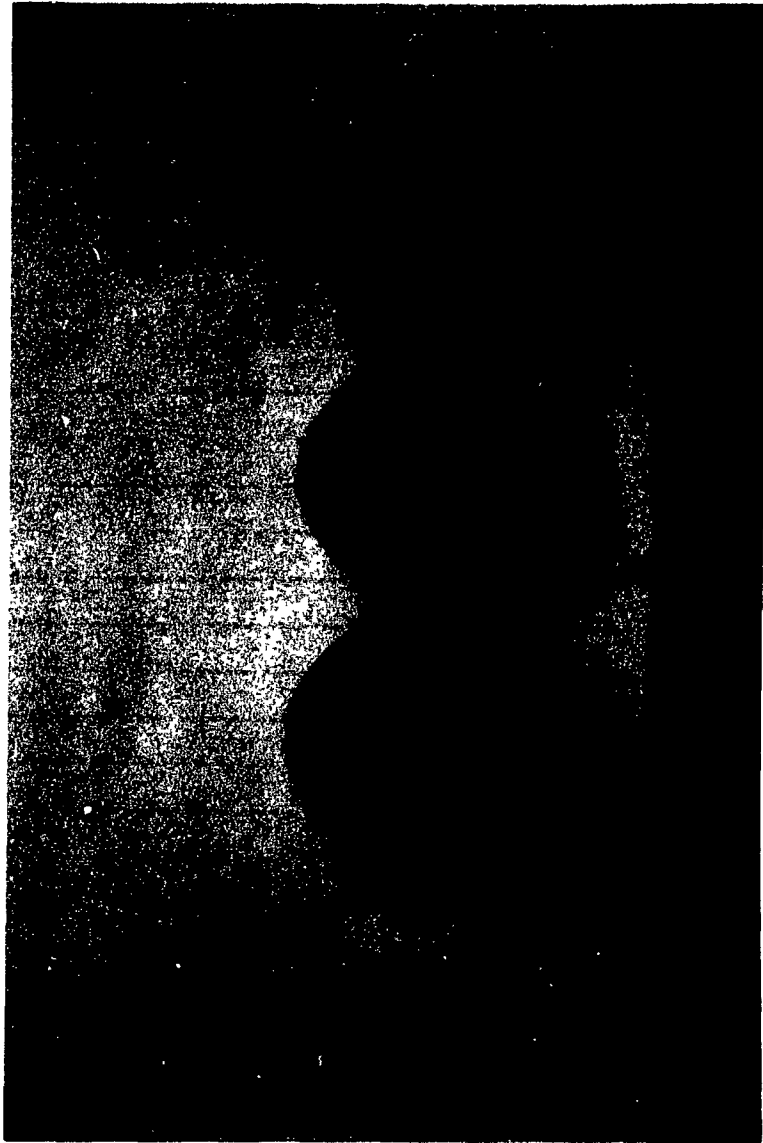
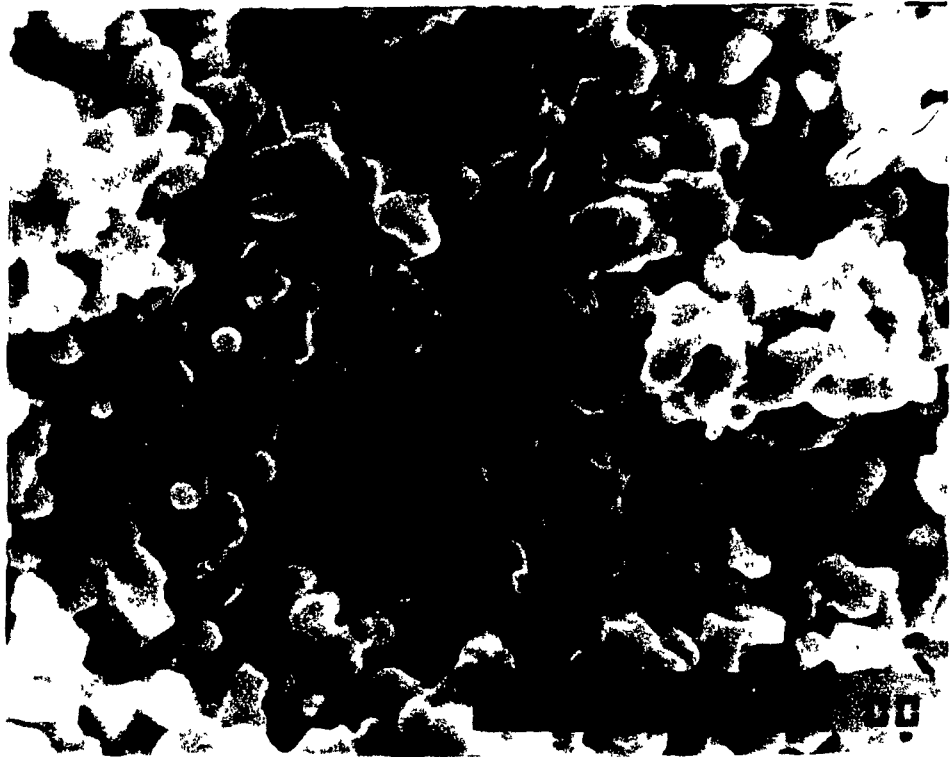


Figure 5-1 The Flow Chart of Fabricating TaC Cathode Ring



*a*                      *b*                      *c*                      *d*

Figure 5-2 The Rings in Different Fabrication Stages



**Figure 5-3**      **The Microstructure of the Rings (SEM)**

## B. Experimental Conditions

In order to clearly identify the behavior of the electrode material - TaC in the plasma torch, it was necessary at the beginning to use operating conditions which allow stable and reproducible operation of the experiments. The conditions which are summarized in Table 5-4 were used successfully by both Szente (1986) and Habelrh (1988), so they were used in this study.

The installation of the cathode ring and the anode tip is shown in Figure 3-3 in which it is seen that the ring was mounted in a copper holder. Ceramic material with high electrical resistance, called 909 Hi-resistance Ceramic Adhesive, maximum operating temperature is 1800 K, made by Contronics Corp, was used to cover the internal copper surface of the holder for insulation, and the whole anode tube, except the working tip made of TaC+Al or Ta, (Cu tip was an integral part of the tube) was also covered with the same ceramic

The distance between the anode tip and the internal surface of the cathode ring was 4 mm which avoids the effects of cathode jets while giving a reasonably low arc voltages.

## C. Results of Experiments

Using the sintered TaC cathodes and copper anodes, nine experiments were carried out under the conditions of Table 5-4. The longest one ran only five minutes. The serious instability of the arc voltage and the fluctuation of the arc velocity caused the stopping of these experiments,

After the experiments it was clearly observed that the cathode ring was cracked and fractured, as shown in Figure 5-4 and Figure 5-5. The internal surface of the ring had melted which indicated that the operating temperature was definitely over 4135 K, the melting point of TaC. The directions of cracking seemed mainly circumferential and axial. The longer the test ran, the more severe was the cracking

**Table 5-4      The Experimental Conditions**

Variables	Specification	
Main Plasma gas	Argon	Purity 99.998 %
Gas Flow Rate	15-20	L/min T= 293 K
Arc Current	100	A
Pressure	1.1	Atm
Magnetic Field	1000	Gauss
Coolant	Cold water	
Rate of Cooling Water	15-20	L/min Cathode
	10-15	L/min Anode
	4	L/min Reactor Walls
Degree of Vacuum	- 100	kPa + 5 min Purging with Ar.

It was very clear that thermal shock and poor thermal conductivity caused the failure of the cathode ring. Increasing of rate of cooling made no difference. In order to minimize the shock, a graphite coating was put onto the working surface of the cathode ring to delay the changing of temperature gradient. This did not improve the situation.

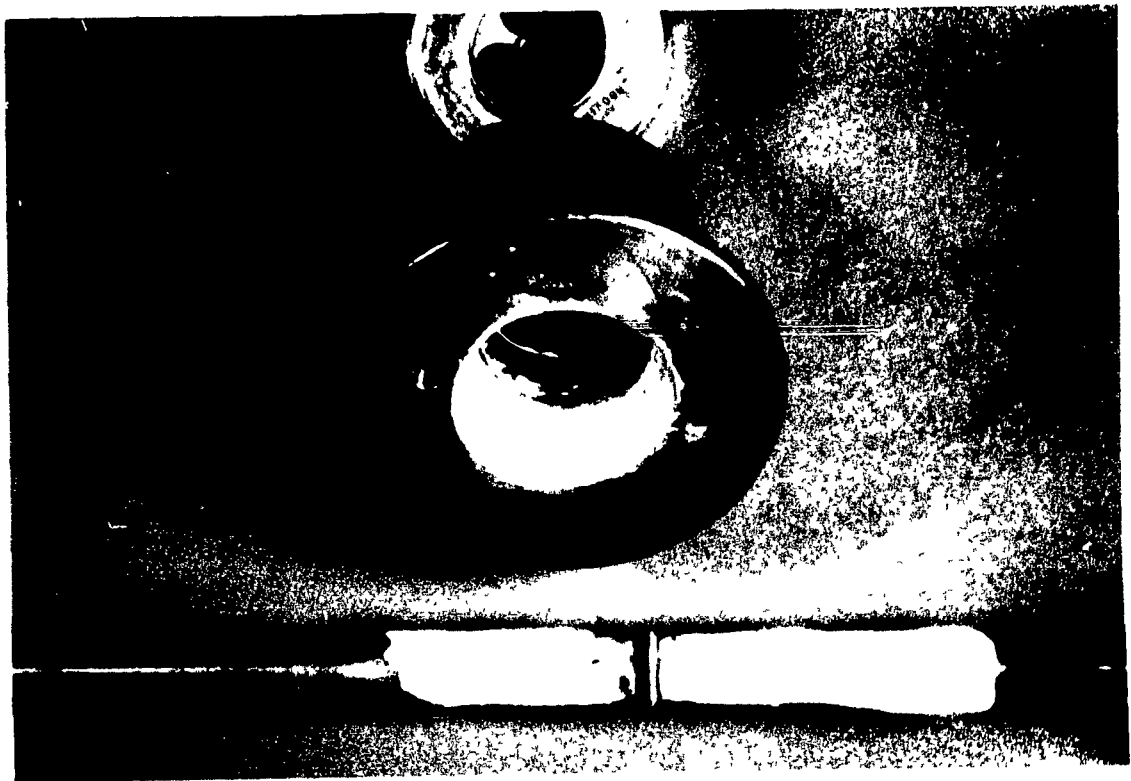


**Figure 5-4** The Photographs of a Cathode Ring and a Copper Anode After Testing



**Figure 5-5** The Fractured Parts of a Pure TaC Cathode Ring

### 5.3 Basic Failure Analysis

From the above results it was realized that no matter how the electrodes are cooled, there always exists a very sharp temperature gradient close to the working surface region of the electrodes where serious stress-strain fields will be produced. These may cause the crack and failure of electrodes. The plasma temperature can not be reduced if an arc is to be maintained.

#### A. Temperature Cycling and Gradient

In order to analyze the reasons of the thermal failure, the temperature field in the body of electrodes should be examined first; This can be expressed in polar coordinates for our electrode ring, shown in Figure 3-3, as follows

$$\frac{1}{r} \frac{\partial}{\partial r} \left( \kappa r \frac{\partial T}{\partial r} \right) + \frac{1}{r^2} \frac{\partial}{\partial \phi} \left( \kappa \frac{\partial T}{\partial \phi} \right) + \frac{\partial}{\partial z} \left( \kappa \frac{\partial T}{\partial z} \right) + \dot{q} = \frac{1}{\alpha} \frac{\partial T}{\partial t} \quad (5-5)$$

where  $T$  is temperature,  $t$  is time,  $\dot{q}$  is heat generation per unit volume and unit time,  $\kappa$  is the thermal conductivity,  $\alpha$  is the thermal diffusivity and  $r, \phi$  and  $z$  are coordinates of a point of the object in polar coordinates.

Obviously, the biggest difficulty of solving the equation (5-5) is that in our plasma torch the temperature field is a strong function of time and position. On one side of the electrode ring there is cold cooling water close to room temperature and on the other side, the working surface of the ring, the temperature is elevated by the plasma arc to thousands of degrees. The thickness of the ring is only around 10 mm. The applied external magnetic field drives the arc running along the surface with high rotational velocity (about 200 cycles per second), and at the spot of the arc root, the temperature can be over 10,000 K. It was demonstrated in the work of other researchers (Szente, 1986 and Habelrih, 1988) that the rest of the surface is quickly cooled down by

passing gas and heat conduction to colder part of the ring. Therefore it is clearly indicated that there exists a very sharp temperature gradient and a severe temperature cycling at the surface of electrodes in the plasma torch.

### B. Thermo-Mechanical Failure of the Electrode Ring

It is known that the temperature and stress-strain fields in a solid medium are (in general) coupled. If it is assumed that the temperature field is independent of time the temperature field is determined from equation (5-5). For preliminary estimation of stress distribution on the cathode ring in the elastic range (this is reasonable for most brittle materials and TaC is very brittle) it may be found that the stress distribution in the cathode ring caused by the temperature gradient can be expressed, in polar coordinates, as

$$\sigma_r = \frac{\alpha_T E}{r^2} \left( \frac{r^2 - r_1^2}{r_2^2 - r_1^2} \int_{r_1}^{r_2} (T - T_0) r \, dr - \int_{r_1}^r (T - T_0) r \, dr \right) \quad (5-6)$$

$$\sigma_\phi = \frac{\alpha_T E}{r^2} \left( \frac{r^2 + r_1^2}{r_2^2 - r_1^2} \int_{r_1}^{r_2} (T - T_0) r \, dr - \int_{r_1}^r (T - T_0) r \, dr - (T - T_0) r^2 \right) \quad (5-7)$$

where  $\sigma_r$ ,  $\sigma_\phi$  are stresses in radial and tangential directions, respectively, E is Young's modulus,  $\alpha_T$  is the coefficient of thermal expansion and  $T_0$  is an initial temperature.

From the equation (5-7) it is seen that  $\sigma_\phi$  is a strong function of temperature  $T(r, \phi, z, t)$ . Especially at  $r = r_1$  i.e. at the internal surface, the second term on the right side of the (5-7) is zero and the first term will be relatively small because of rapid reduction of temperature away from the working surface inside of the ring. In order to clearly see the relation between stress and temperature the following approximate expression may be given:

$$\sigma_{\phi} \approx -\alpha_T E (T - T_0) \quad (5-8)$$

which means when  $T$  sharply increases and is much greater than the initial  $T_0$ , and there exist very high compressive stresses at the thin surface layer. As  $\sigma_{\phi}$  increases up to yield limits with  $T$  plastic deformation for most ductile material will release the  $\sigma_{\phi}$  towards a new equilibrium of forces. If this equilibrium can not be maintained due to the continued increasing of  $T$  and  $\sigma_{\phi}$ , the material will fail. Of course, when the temperature is extremely high (under the melting point of the electrode materials) the above equations should be corrected by considering thermal plasticity according to the physical and mechanical properties of the materials

### C. Conclusion

After the above qualitative discussion we have the following conclusions:

- i. Pure TaC electrodes are so brittle that they can not endure the thermal shock of plasma arc.
- ii. TaC material can not be used for plasma electrodes, unless a method could be found to control the gradient of temperature in the body of electrodes, especially close to the working surface, to acceptable levels.
- iii. A technique must be found to change the properties of this kind of electrode material, making it more ductile and able to withstand thermal shock. Work was thus started on composite TaC+Al electrodes which were much more ductile. Reactions between the aluminium and the  $TiCl_4$  could result in contamination of the products in a titanium producing process, however such contamination would not be a serious problem, since aluminium is a common alloying element for titanium.

## **CHAPTER 6.**

### **EXPERIMENTS WITH TaC+Al ELECTRODES**

---

#### **6.1 Preparation of TaC+Al Electrodes**

##### **A. Fabrication of TaC+Al Electrodes**

As mentioned in the previous chapter, the thermo-mechanical properties of TaC electrodes were modified by infiltrating these with aluminium. The basic process shown in Figure 5-1 was modified to that shown in Figure 6-1.

##### **B. The Properties of TaC+Al Material**

The basic mechanical properties of TaC+Al material, measured by Noranda Technology Center, are listed in Table 6-1.

The new material is no longer brittle, indicated by the large elongation, but rather ductile like aluminium, and easily machinable.

The micrograph of the new material is shown in Figure 6-2, in which the black areas are completely full of aluminium. Comparing Figure 6-2 to Figure 5-4, even though the scales are slightly different, it may be noted that infiltrating of aluminium has greatly changed the microstructure of the material. The TaC particles have increased considerably in size, they have been packed densely and uniformly, and have acquired extremely regular shapes.

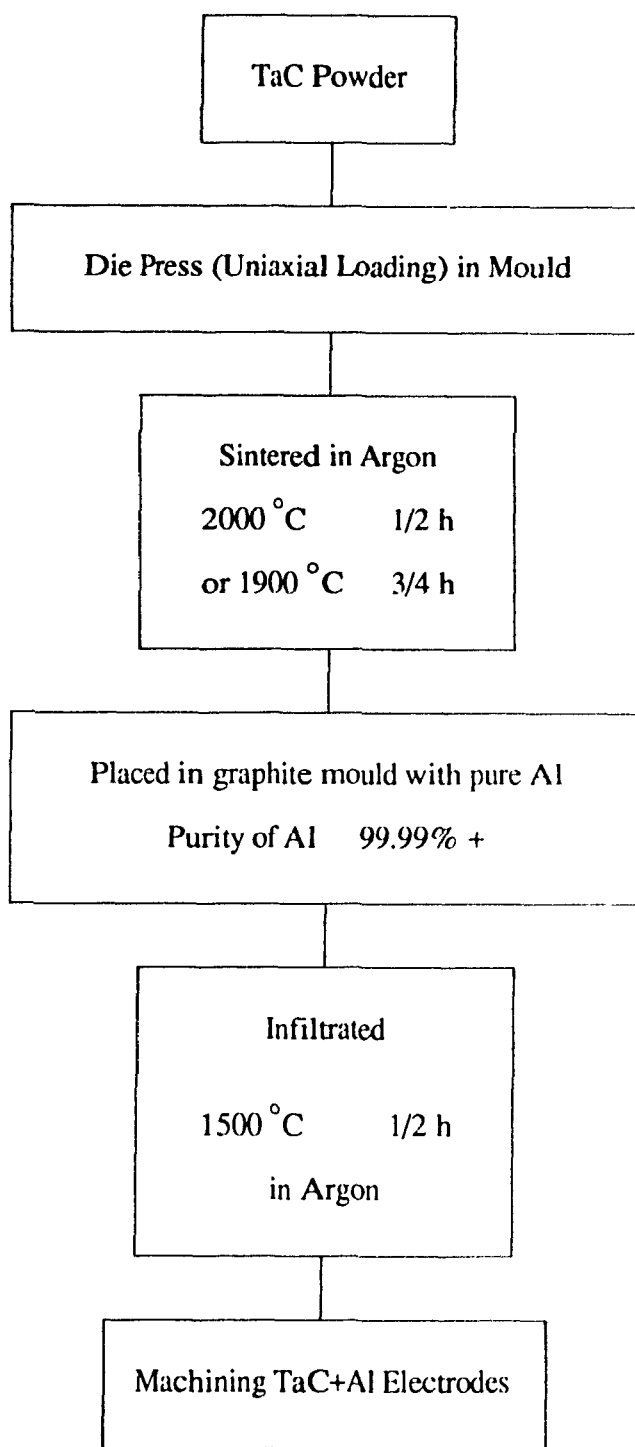


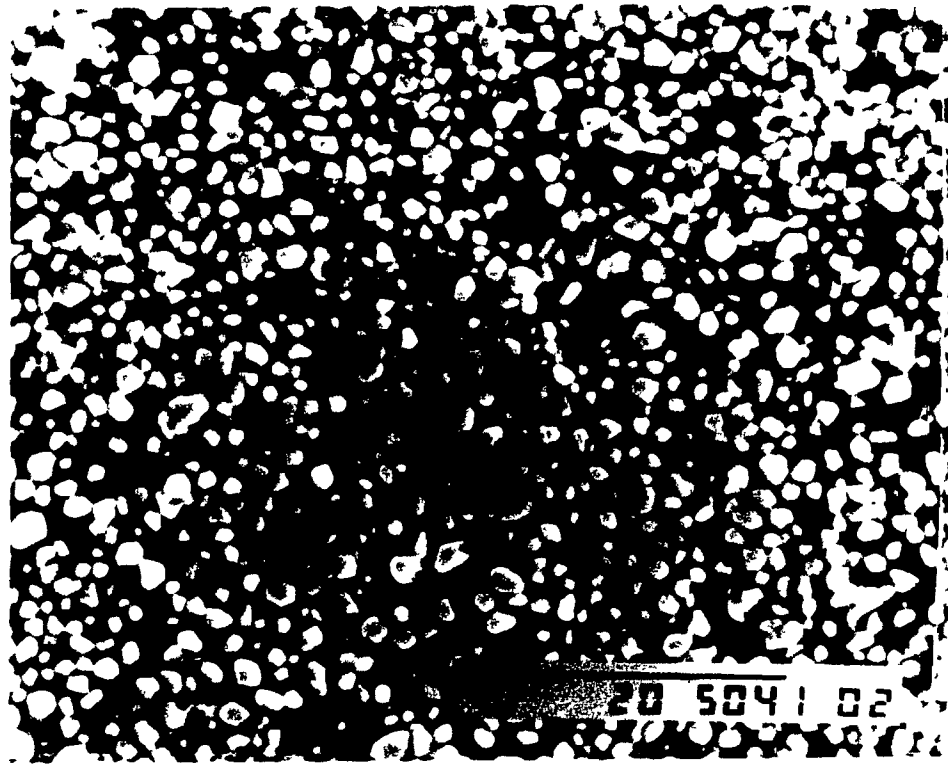
Figure 6-1 The Flow Chart of TaC+Al Electrodes Fabrication

**Table 6-1      The Properties of TaC+Al Material**

---

Ceramic Volume Fraction	55 %
Electrical Resistivity	$9.6 \times 10^{-6} \Omega \text{ cm}$
Thermal Diffusivity	0.275 cm/sec at 291 K
Yield Strength (0.1 %)	80 Mpa
Ultimate Tensile Strength	435 Mpa
Maximum Elongation	9 %
Ultimate Compressive Strength	600 Mpa
Hardness (Rockwell A, 60 kg)	53

---

**Figure 6-2      The Micrograph of a TaC+Al Electrode**

## 6.2 TaC+Al Electrodes in Argon Plasma Gas

### A. Results

In order to demonstrate the basic behavior of the newly developed material TaC+Al, some preliminary experiments were carried out with pure argon gas which would be used to dilute the  $TiCl_4$ . The experimental conditions were listed in Table 6-2. In these experiments the anodes were normally copper. This was a temporary choice because copper is not suitable for  $TiCl_4$  gas. Therefore in  $TiCl_4$  experiments, both anode tips and cathode rings were made of TaC+Al. The results are shown in Table 6-3. The photograph of the cathode ring and anode tip (the small piece) of Test No. 9004 after a test of more than one hour is shown in Figure 6-3. The microstructure of the cathode ring of Test No. 8906 after one hour of operation is shown in Figure 6-4, in which the left side part is an unaffected region close to the outside surface of the cathode ring; the right side part is taken from a zone close to the working surface, strongly affected by the arc.

### B. Discussion

The voltage responses of the plasma arc generated with the new electrodes were very stable throughout the experiments as was the arc current. The average voltage changed somewhat from run to run, possibly due to changes from electrode to electrode and the differences in the gas flow rate. The differences in the velocity of the arc was partially because of changes in electrode composition and density and the changes of gas density. However, it can be seen from Table 6-3 that the average erosion rates of the cathode rings were acceptably low. It was found that the erosion rates are quite sensitive to electrode density. It is noted that the cathode ring of Test No. 9001 had a much lower density, i.e. more aluminium. This would give more Al in the arc as vapor (thus

reducing the voltage) and would also suggest a higher erosion rate because Al is much easier to melt and vaporize than TaC.

From Figure 6-3 and Figure 6-4 it can be seen that the microstructure of the material still remained relatively uniform, even though the surface was very rough due to local melting caused by the attack of the arc. Finally the tests demonstrated stable operation for more than one hour giving a good deal of confidence in this new material.

**Table 6-2 Experimental Conditions for TaC+Al  
Electrodes in Argon Plasma**

No.	Gas Flow R	Gas T	P	Current	B	Water	
	(L/min)	(C)	(atm)	(A)	(G)	Anode	Cathode
8904	14.00	297	1.00	100	1000	8.71	10.6
8906	15.00	298	1.00	100	1000	8.71	10.6
9001	8.12	298	1.07	100	1000	7.57	13.2
9004	8.12	298	1.07	100	1000	7.57	13.2
9028	15.43	297	1.07	100	1000	7.57	13.2

**Table 6-3      The Results of TaC+Al Cathode Rings in Argon Gas**

No.	Density (g/cm <sup>3</sup> )	Voltage (V)	Velocity (m/s)	Erosion Rate (μg/C)	Time (min)
8904	(63%TaC)*	25	-	-	5
8906	(65%TaC)*	26	-	-	60
9001	5.760	23	13.85	4.39	49
9004	7.013	24	-	1.31	61
9026	7.053	30	13.57	-	15
9027	6.914	29	13.57	-	6.3
9028	6.909	25	36.28	1.55	30.2

\* The density in g/cm<sup>3</sup> was not measured;

- The data not available

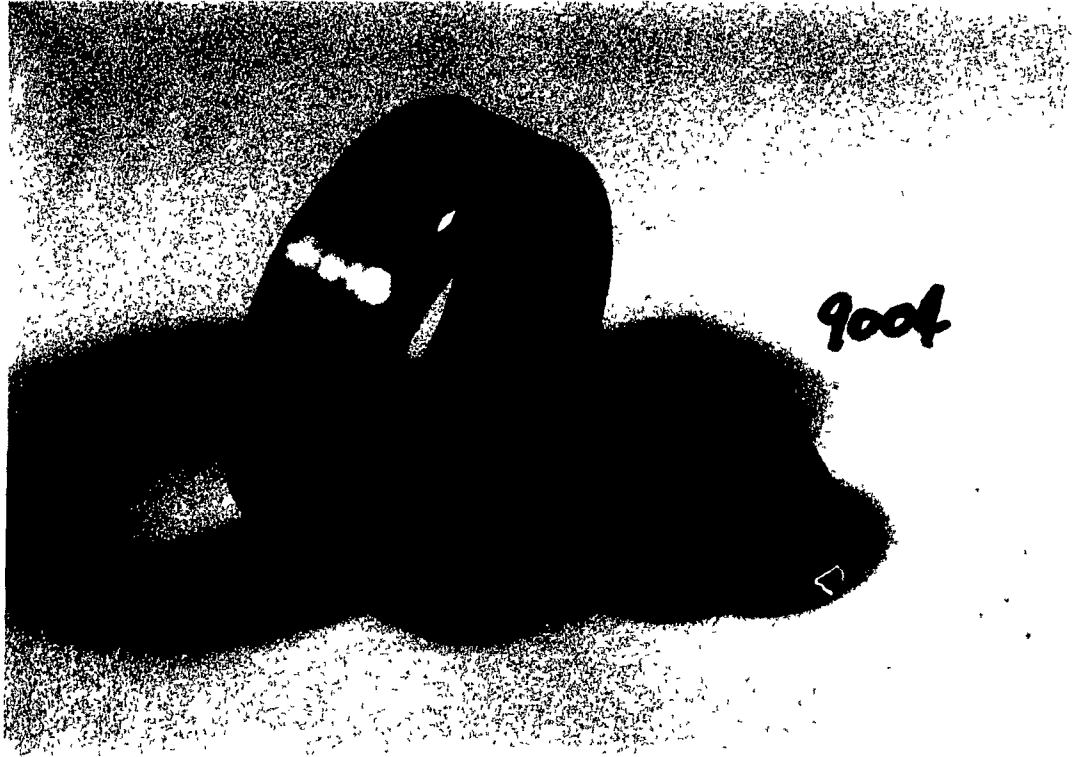


Figure 6-3 The Photograph of a Ring and a Tip After a One Hour Test

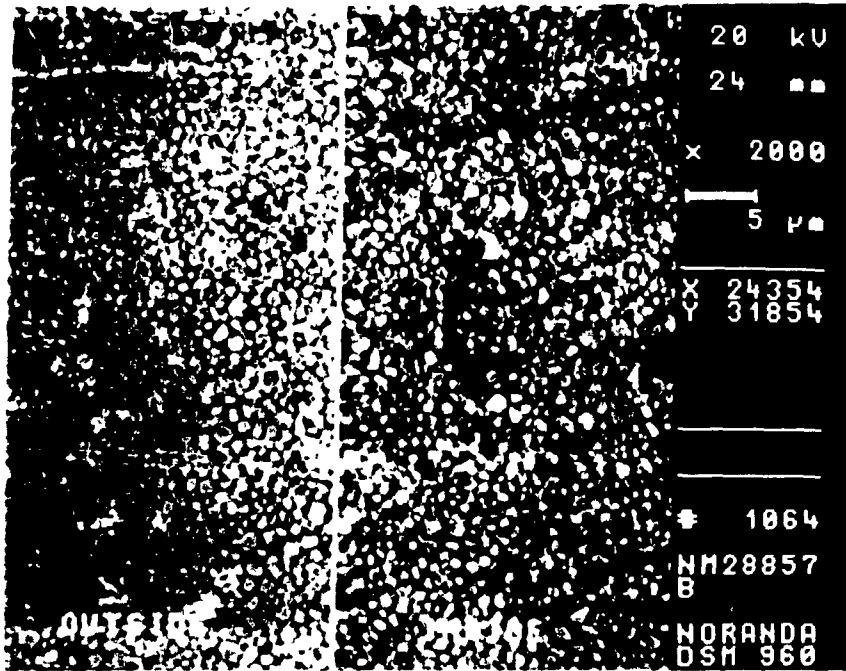


Figure 6-4 The Microstructure of TaC+Al After a One Hour Test

### 6.3 TaC+Al Electrodes in $\text{TiCl}_4$ + Argon Plasma Gases

#### A. Experimental Conditions

According to the experience of the above pioneering and preliminary experiments the following experimental conditions were used for the all experiments with  $\text{TiCl}_4$  + argon plasma gases:

**Table 6-4 Operating Conditions for  $\text{TiCl}_4$  + Argon Plasma Gases**

Arc current	=	100	A
Flow rate of argon	=	15	L/min
Magnetic Field	=	1000	Gauss
Pressure in reactor	=	1 - 1.1	atm
Flow rate of cooling			
Cathode	=	13.2	L/min
Anode	=	7.57	L/min
Temp. of cooling water	=	358-363	K

#### B. The Features of the Arc Voltage

A great deal of attention was paid to the arc voltage and its stability since this determines not only the stability of the plasma arc but is a good indicator of the behavior of the arc root at the electrode surface.

More than twenty experiments were done to investigate the behavior of the arc voltage. The results corresponding to different  $\text{TiCl}_4$  concentrations are summarized in Table 6-5, as follows

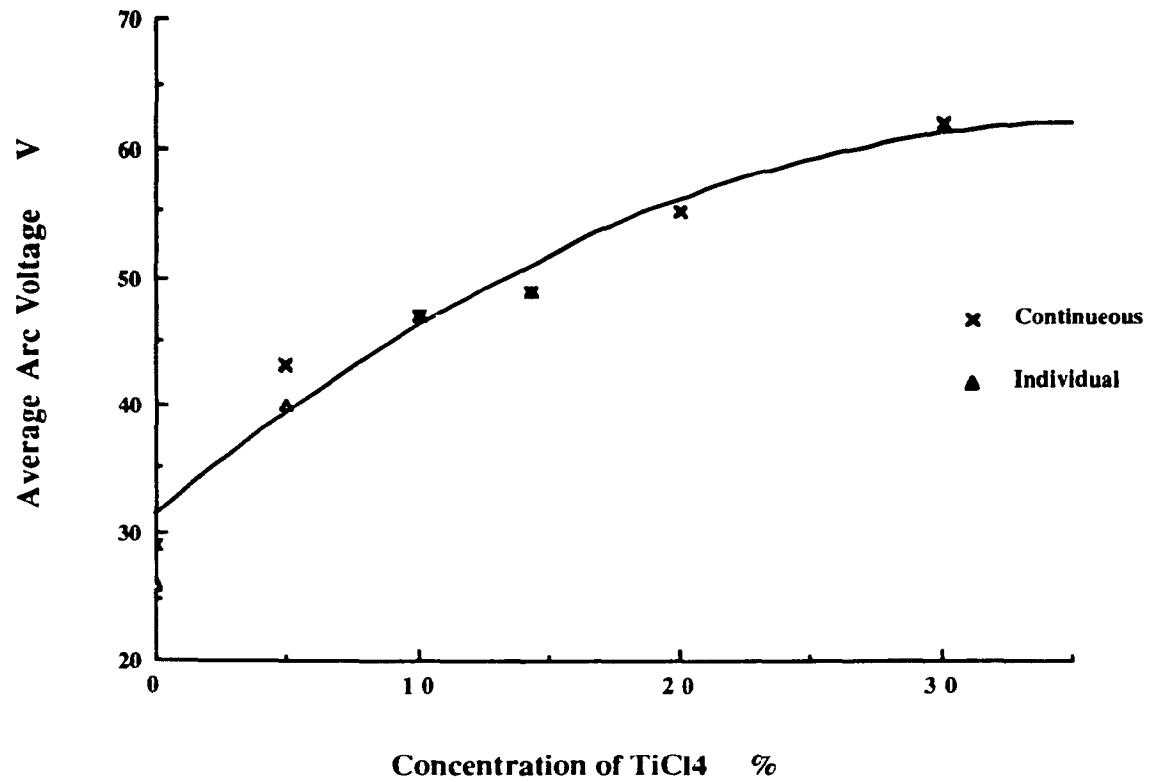
**Table 6-5 The Arc Voltage vs TiCl<sub>4</sub> Concentration**

No.	Concentration of TiCl <sub>4</sub> (Volume %)	Average Voltage (V)	Time (min)
9028	0.0	25	30.2
9006	2.5	35	6.5
9025	5.0	40	20.0
9012	8.0	45	4.5
9024	10.0	46	20.0
9023	14.3	50	20.5
9027	20.0	55	2.6
9027	30.1	62	4.0

The voltage - concentration data of Table 6-5 have been plotted in Figure 6-5 in which the solid line curve presents the fit expression. It is shown that the voltage of the arc appears to increase as a quadratic function (the correlation coefficient  $R^2 = 0.96$ ) of the concentration of TiCl<sub>4</sub>. This increase can be explained by the fact that the decomposition of more TiCl<sub>4</sub> requires additional energy and thus increases the arc voltage.

The crosses in Figure 6-5, named "Continuous" are the result of a single run in which the concentration of TiCl<sub>4</sub> was changed in a stepwise fashion (such as Run 9026 and 9027). The triangles represent the results of the runs which were conducted at single fixed concentrations of TiCl<sub>4</sub>.

Figure 6-5 Average Arc Voltage vs Concentration of TiCl4



$$V = 31.334 + 1.7112C - 2.3753e-2C^2 \quad R^2 = 0.960$$

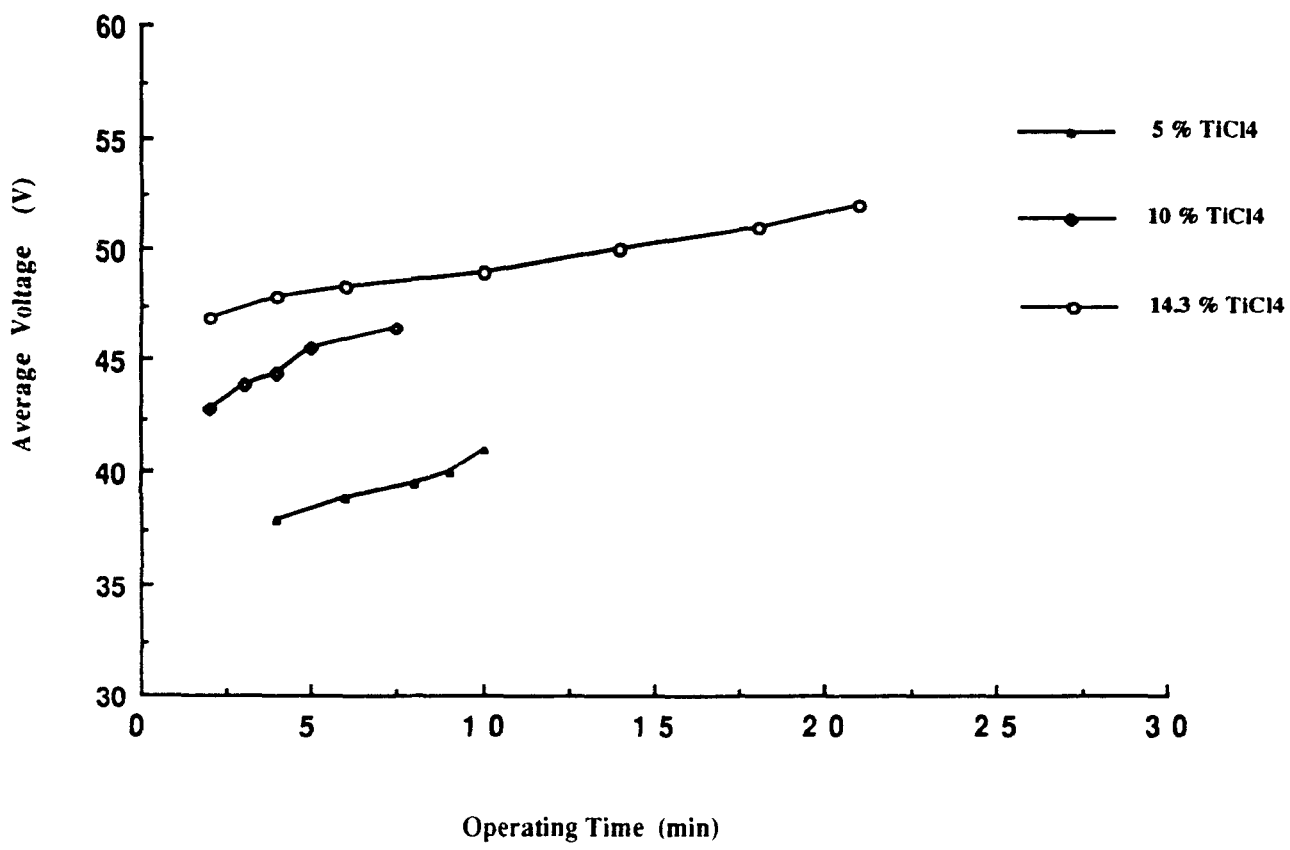
The reproducibility of the experiments was also investigated and the results of average voltages for runs at a concentration 14.3%  $\text{TiCl}_4$  are listed in Table 6-6. These values are obtained by averaging peak to peak value of voltage over the time of the experiments. The reproducibility of voltage appears quite good.

Figure 6-6 shows that the short term average plasma voltages as a function of the operating time and illustrates that even at time scales at which the concentration should have achieved steady state (after about a minute) the average voltage still increases. This phenomenon could be interpreted as due to the deterioration of the electrodes in which the surface quality of the electrodes and the width of the gap between the electrodes were changed.

**Table 6-6 Reproducibility of the Arc Voltage**

No.	Concentration. $\text{TiCl}_4$ (Volume %)	Average Voltage (V)	Time (min)
9015	14.3	48	4.0
9013	14.3	48	6.0
9008	14.0	46.5	10.0
9023	14.3	50.0	20.5

Figure 6-6 The Feature of Average Voltage vs Operating Time



The typical evolution of the arc voltage with the operating time is shown in the strip chart recording of Figure 6-7 for the test numbered as 9023. In this figure the concentration of  $\text{TiCl}_4$  was 14.3 %. When  $\text{TiCl}_4$  vapor was first fed to the main argon flow, the composition of plasma gases changed rapidly and for the first few seconds it was not uniform. The voltage showed a short fluctuating phase, and the actual length of this fluctuating phase depended mainly on the mixing process between  $\text{TiCl}_4$  and argon (sometime more than one minute). Once the mixing process was completed and the composition of plasma gases became uniform again the arc voltage appeared to be much more stable; then the range of fluctuation was only about 1 - 4 V while the operating voltage was 35 - 62 V. The level of fluctuations was greatest at the lowest  $\text{TiCl}_4$  concentration due to the pulsing nature of the peristaltic pump at low flow rates.

In summary, the above results show that stable plasma arcs were produced with up to 30 % concentration of  $\text{TiCl}_4$  in argon gas.

### C. Weight Loss and Erosion Rate

In order to characterize the deterioration of electrodes working in  $\text{TiCl}_4$  + argon plasma gases the weight loss and average erosion rate of the electrodes were measured. The results are summarized in Table 6-7. It should be noted that in all experiments the arc was ignited first in pure argon and then  $\text{TiCl}_4$  gas was fed into the reactor; this was done for ease of arc ignition. In the calculation of the weight loss and the erosion rate the influence of this short period of argon running was subtracted by measuring the time of this period and using experimental erosion data of the pure argon experiments. The results in Table 6-7 are the corrected results.

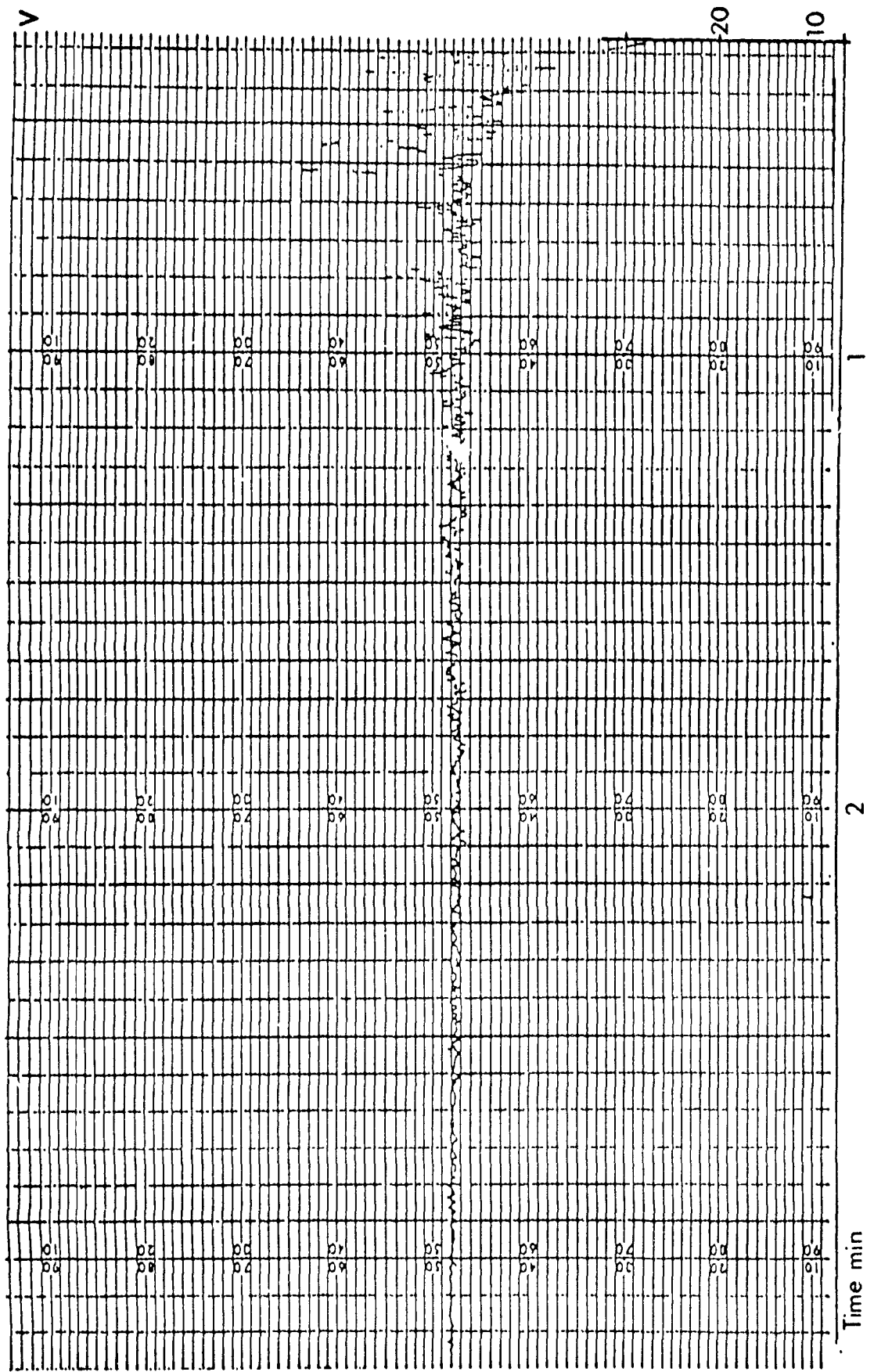


Figure 6-7 The Response of Voltage During 14% TiCl<sub>4</sub> Gas Testing

Table 6-7 Weight loss and Erosion Rate of Electrodes

No.	Concentration	Time (sec)	Weight Loss		Erosion Rate	
	TiCl <sub>4</sub>		(g)		(μg/C)	
	(Volume %)		Cathode	Anode	Cathode	Anode
9006	2.51	330	0.41	0.42	9.37	11.45
9007	2.51	390	0.31	0.08	7.20	1.76
9022	5.12	240	0.50	0.89	20.82	37.05
9019	4.99	360	0.68	0.28	18.83	7.85
9016	5.02	600	0.76	0.55	12.59	9.17
9025	5.16	1200	1.79	2.10	14.71	17.39*
9012	8.00	270	0.43	0.45	14.64	16.33
9020	10.01	250	0.58	0.72	23.25	28.89
9018	10.00	365	0.80	0.48	21.83	13.15
9014	10.00	600	1.10	0.84	18.27	14.01
9021	10.10	645	1.64	3.16	23.51	45.45*
9024	10.13	1200	1.94	4.96	16.05	41.29*
9015	14.31	240	0.71	0.42	29.31	17.44
9013	14.30	360	1.00	0.36	27.72	10.05
9008	14.31	600	1.52	1.45	25.12	24.06
9023	14.31	1230	3.07	0.89	24.89	7.24

\* The material of the anode used is pure tantalum instead of TaC+Al.

In this section attention will be only paid to the behavior of the TaC+Al cathodes, even though some data for anodes are listed in Table 6-7. The behavior of the anodes will be presented in a later section.

Table 6-7 shows that

i) The weight loss of the TaC+Al cathode is a function of both operating time and concentration of  $TiCl_4$ , as shown in Figure 6-8 and Figure 6-9. The weight loss appears, in Figure 6-8, to be a linear function of time with different slopes due to different concentrations of  $TiCl_4$  gas. The fitting expressions can be written as

$$WL_{14.3} = 0.06766 + 2.4525 \times 10^{-3} t \quad R^2 = 0.999 \quad (6-1)$$

$$WL_{10} = 0.03874 + 1.9334 \times 10^{-3} t \quad R^2 = 0.992 \quad (6-2)$$

$$WL_5 = 0.06929 + 1.4152 \times 10^{-3} t \quad R^2 = 0.959 \quad (6-3)$$

where the subscripts of WL (Weight Loss) indicate the concentration of  $TiCl_4$  and R is correlation coefficient; the units of weight loss and time are g/s and s, respectively.

The derivatives of the above three equations will give the approximately constant erosion rates corresponding to the different concentration of  $TiCl_4$  gas:

$$\frac{dWL_{14.3}}{dt} = 2.4525 \times 10^{-3} \quad (g/s) \quad (6-4)$$

$$\frac{dWL_{10}}{dt} = 1.9334 \times 10^{-3} \quad (g/s) \quad (6-5)$$

$$\frac{dWL_5}{dt} = 1.4152 \times 10^{-3} \quad (g/s) \quad (6-6)$$

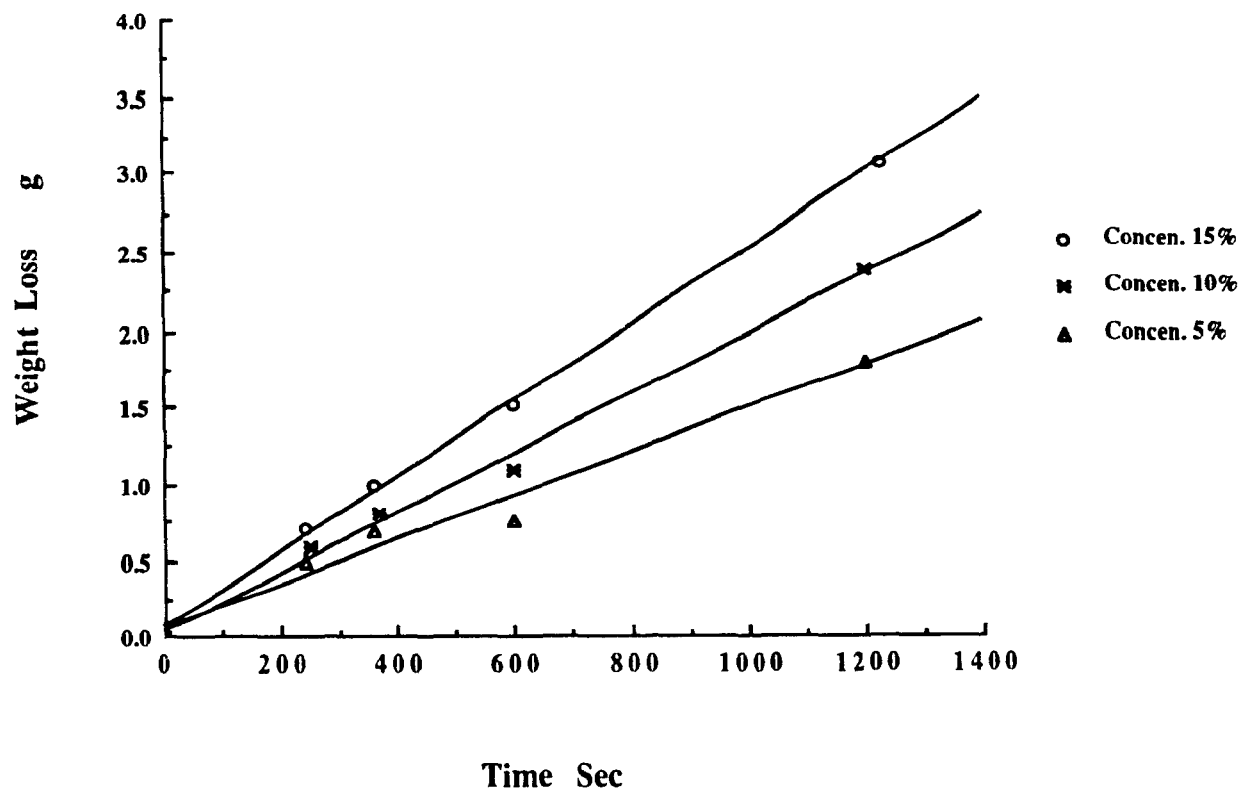


Figure 6-8 The Weight Loss of TaC+Al Cathode in TiCl<sub>4</sub> Plasma

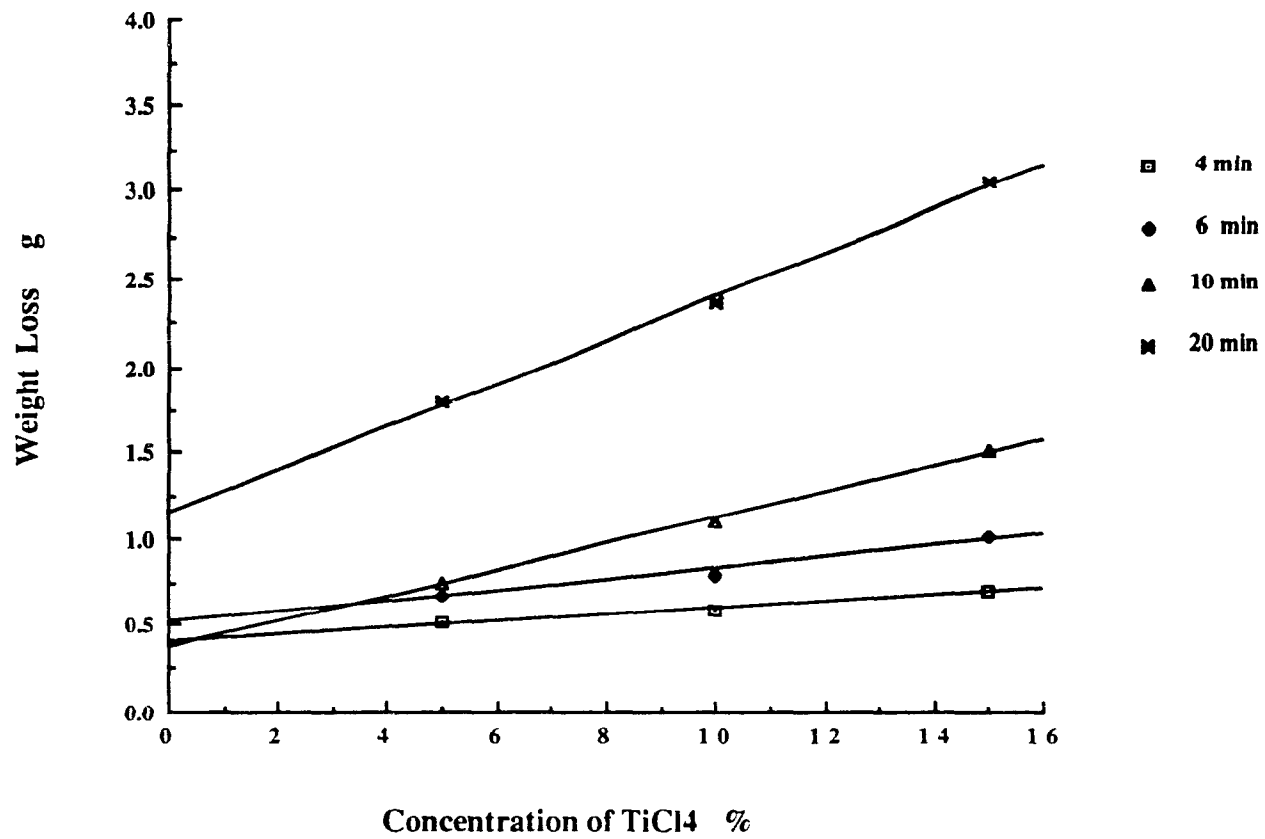


Figure 6-9 The Weight Loss of TaC+Al Cathode vs the Concentration of TiCl4

Furthermore, if the above three expressions (6-4), (6-5), and (6-6) are divided by the value of the current which is fixed as 100 A in all experiments, the three approximate erosion rates can be expressed in  $\mu\text{g}/\text{C}$ , as follows

$$ER_{143} = \frac{dWL_{143}}{dt} = 24.525 \quad (\mu\text{g}/\text{C}) \quad (6-7)$$

$$ER_{10} = \frac{dWL_{10}}{dt} = 19.334 \quad (\mu\text{g}/\text{C}) \quad (6-8)$$

$$ER_5 = \frac{dWL_5}{dt} = 14.152 \quad (\mu\text{g}/\text{C}) \quad (6-9)$$

where C means Coulomb and  $\mu\text{g}$  means micro gram, the subscripts of ER (Erosion Rate) represent the concentrations of  $\text{TiCl}_4$ .

These mean erosion rates are quite close to the erosion rates calculated from individual experiments if the runs were relatively long.

Figure 6-9 shows that the weight loss of the TaC+Al cathode is a linear function of the concentrations of  $\text{TiCl}_4$ , and that for different running periods of experiments the expression is different.

ii) Although the measured erosion rate computed in Table 6-7 is not an instantaneous value but the average value over a run, some use can still be made of the data, which seem consistent with the analysis of the weight loss. It is also observed from Figure 6-10 that this average rate approaches a constant value, in other words, is independent of operation time, for each concentration of  $\text{TiCl}_4$  but is initially higher. The initial higher rate may be attributed to chemical reaction at regions of high initial aluminium concentration at the electrode surface but not necessarily at the arc root. It may also be a result of the initial arc instability due to the initial unsteady flow rate of  $\text{TiCl}_4$  into the system. This is corroborated by the initial portion of the arc voltage versus time curves shown in Figure 6-7.

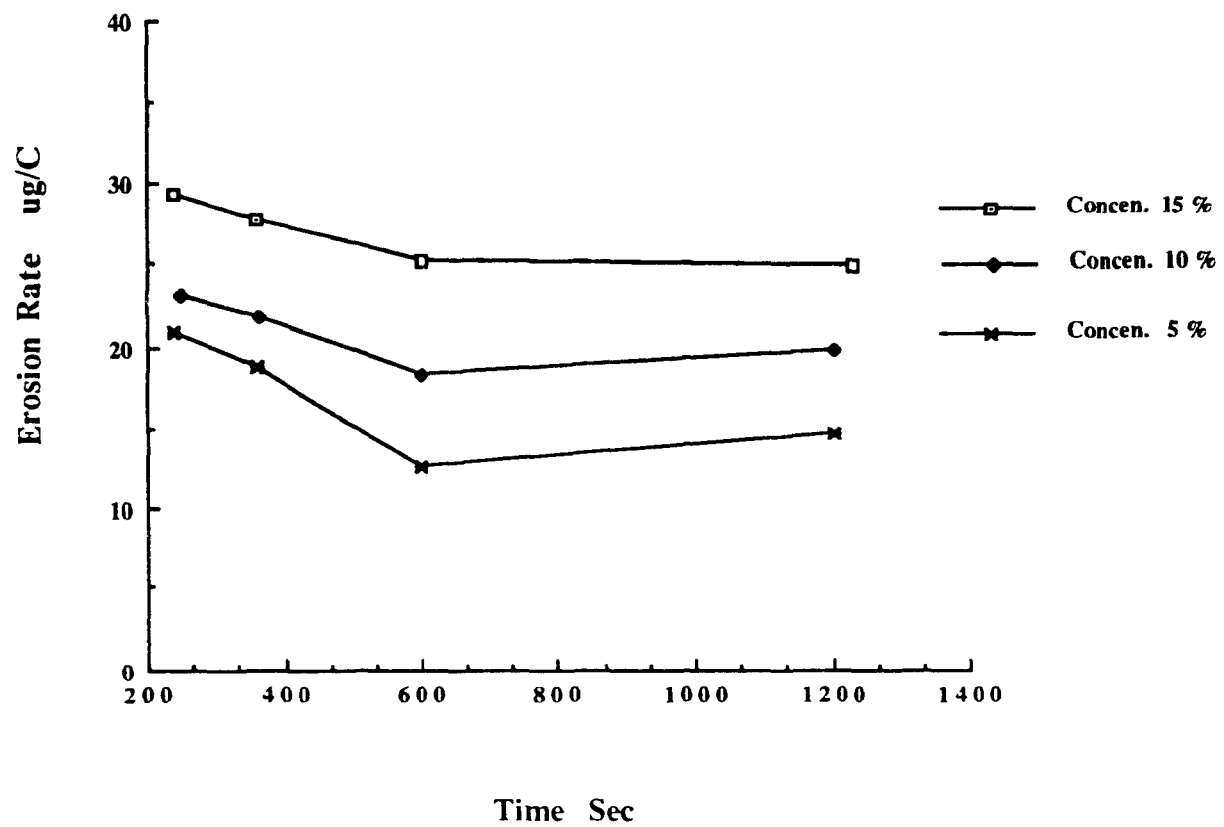


Figure 6-10 The Erosion Rate of TaC+Al Cathode in  $\text{TiCl}_4$  Plasma

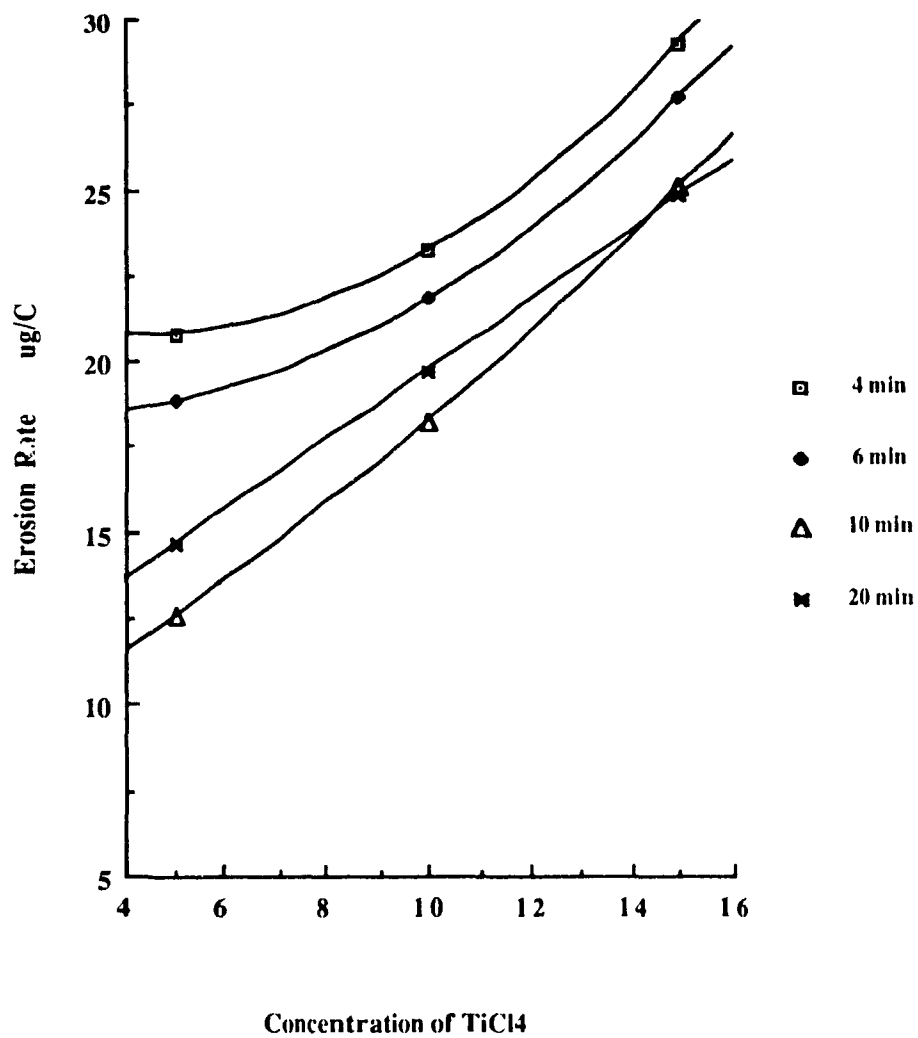
iii) A cross plot of the mean erosion rate data versus the  $\text{TiCl}_4$  concentration with time as a parameter is given in Figure 6-11. For the short time runs, the erosion rates versus the concentrations are a quite non-linear function, shown by the equations (A) and (B) in Figure 6-11, whereas for long time runs, which are more characteristic of steady state operation, the curves becomes linear, indicated by the equation (D) in Figure 6-11. As mentioned above, the behavior of erosion rate in a short time run was strongly affected by the initial instability of  $\text{TiCl}_4$  flow rate.

#### D. Arc Velocity

The measured data on mean arc velocity as a function of  $\text{TiCl}_4$  concentration at constant magnetic field are summarized in Table 6-8 and have been plotted in Figure 6-12. The velocity of Run 9028 has not been plotted for the reasons discussed below. The velocities show more scatter than the voltage data because velocity data could only be taken during the initial portion of the runs when the window was still clear of solid reaction products.

Figure 6-12 shows that the arc velocity is about 13 m/s in pure argon. The velocity increases and then decreases as the titanium tetrachloride concentration increases. The low initial velocity may be associated with surface drag at the cathode as was found by Szente (1988) for pure argon and helium on copper cathodes. Once concentrations of more than a few hundred ppm of a contaminant are present in argon, the surface drag is reduced and the arc behavior is determined primarily by the bulk gas through which the arc passes and not by surface effects. The high velocity of Run 9028, in Table 6-3, may be due to slight contamination of the argon by  $\text{TiCl}_4$  in that run. This would reduce surface drag and permit a high arc velocity. Because of the operational limits of the titanium tetrachloride feeder, no experiments could be done to investigate the arc behavior at very low titanium tetrachloride concentrations.

Figure 6-11 Erosion Rate as a Function of TiCl4 Concentration at Different Times



$$Er_4 = 22.018 - 0.60320C + 7.2640e-2C^2 \quad (A)$$

$$Er_6 = 18.709 - 0.26350C + 5.7620e-2C^2 \quad (B)$$

$$Er_{10} = 8.0870 + 0.78330C + 2.3500e-2C^2 \quad (C)$$

$$Er_{20} = 9.5897 + 1.0185C \quad (D)$$

**Table 6-8      The Arc Velocities in Different Conditions**

No.	Concentration (%)	Velocities (m/s)			Time (sec)
	TiCl <sub>4</sub>	Max	Min	Mean	
9017	14.31	12.07	10.56	11.31	125
9008	14.31	7.60	7.60	7.60	600
9013	14.30	9.10	6.04	7.57	360
9018	10.00	15.08	15.08	15.08	365
9020	10.01	12.41	12.41	12.41	250
9012	8.00	18.97	15.18	17.08	270
9022	5.12	18.99	15.19	17.09	240
9016	5.02	16.79	16.79	16.79	600
9007	2.51	43.21	21.61	32.41	390
9001	0.0	15.02	12.67	13.85	2940
9026	0.0	15.08	12.06	13.57	900
9027	0.0	15.08	12.06	13.57	380

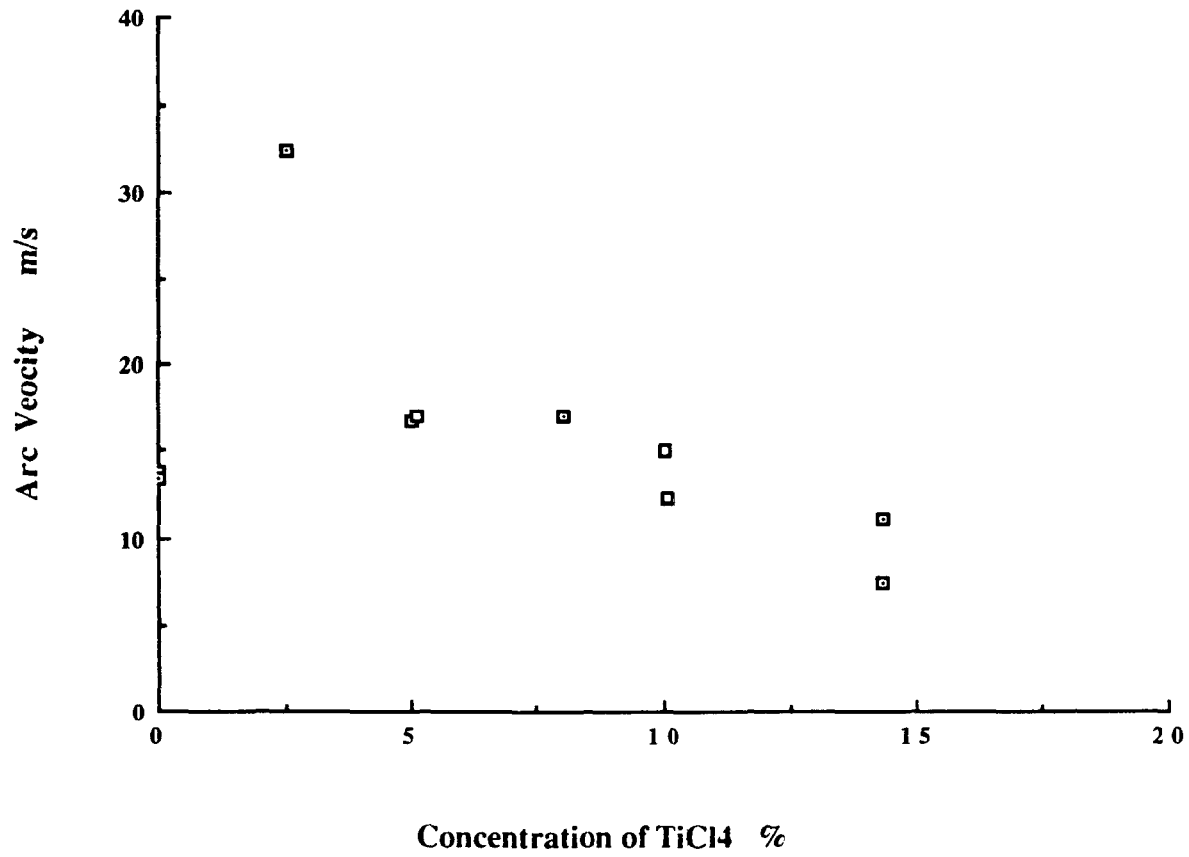


Figure 6-12 Arc Velocity vs TiCl4 Concentration

Figure 6-13 is a logarithmic plot of arc velocity versus  $\text{TiCl}_4$  concentration including only concentrations higher than 2.5%, i.e. under conditions where surface drag is expected to be small and independent of concentration. The least squares regression of velocity on concentration gives:

$$\text{Vel} = 59.35 y^{-0.694} \quad (6-10)$$

where Vel is the arc velocity in m/s and y is the titanium tetrachloride concentration in mole fraction.

A theoretical analysis based on a balance of the Lorentz and drag forces and negligible surface drag, expressed in equations (2-1), (2-2) and (2-4), gives:

$$\text{Vel} \propto \rho^{-0.5} \quad (6-11)$$

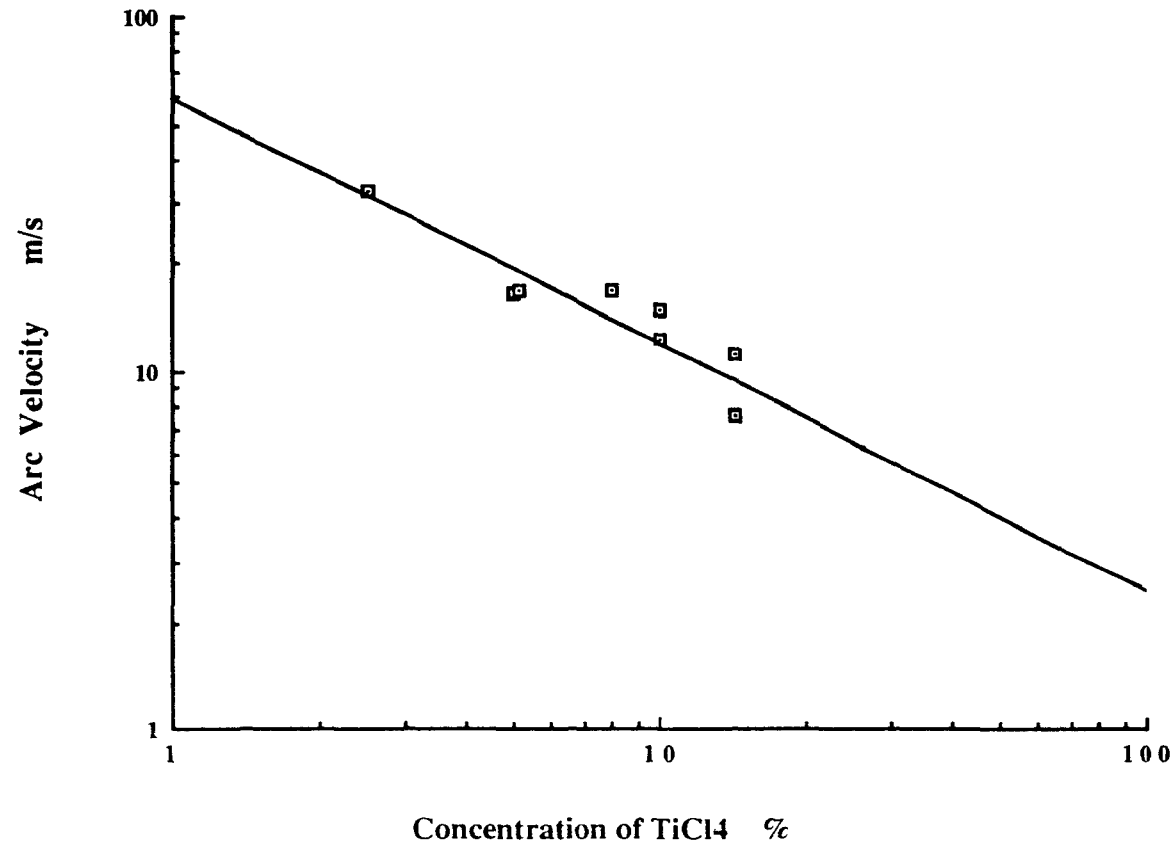
The density of the gas in the reactor between the electrodes will be a function of its titanium tetrachloride concentration. The  $\text{TiCl}_4$  affects the density in two different ways; it directly affects the density because of the higher molecular weight of  $\text{TiCl}_4$  but it also causes an increase in the arc voltage. This would tend to heat the gas and cause a reduction in the density. If it is assumed that the arc efficiency does not change with changing concentration, then the variation of overall gas density with  $\text{TiCl}_4$  molar concentration can be computed from heat balance and molecular weight consideration as:

$$\rho \propto y^{0.45} \quad (6-12)$$

where y is the molar concentration of  $\text{TiCl}_4$ . This is approximately true over a wide range of torch efficiencies, i.e. from 20% to 40% which is expected to be the case here. If we combine equation (6-11) and (6-12) we can obtain:

$$\text{Vel} \propto y^{-0.225} \quad (6-13)$$

Figure 6-13 Arc Velocity as a Function of TiCl4 Concentration



$$\text{Vel} = 59.350 * y^{-0.69352} \quad R^2 = 0.847$$

which suggests that the velocity should decrease as the concentration of  $\text{TiCl}_4$  increases. The model assumes no chemical reaction in the arc which certainly not the case in this work. If there was reaction, the arc would heat the gas to a lower temperature than predicted since the decomposition of  $\text{TiCl}_4$  is endothermic. This suggests that the gas density would decrease more strongly with increasing of  $\text{TiCl}_4$  concentration than is predicted by equation (6-12) meaning that the velocity should decrease more rapidly than predicted by equation (6-13). The experimentally determined dependence of arc velocity on  $\text{TiCl}_4$  given in equation (6-10) above suggests that there was considerable reaction, and thus quenching of the gas, as was observed.

The photographs of the arc in  $\text{TiCl}_4$  (see Figure 6-21 below) corroborate these interpretations since the arc was short and perpendicular to the two electrode surfaces; this is exactly what would be expected if surface drag on the cathode was negligible.

#### E. Effect of Arc Velocity on Erosion Rate

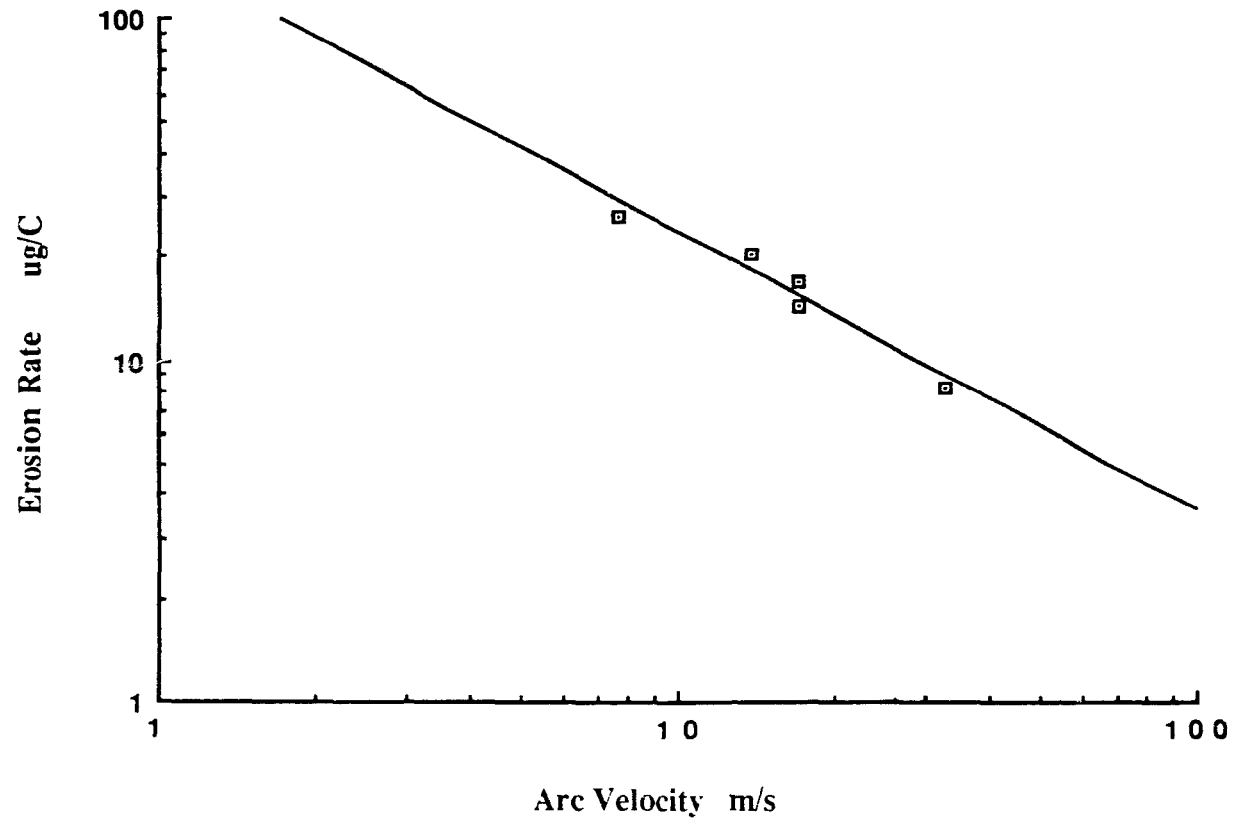
Because the arc velocity changes as the concentration of  $\text{TiCl}_4$  is changed, it is difficult to unambiguously separate the effects of concentration and velocity on the erosion rate. Figure 6-14 is a logarithmic plot of erosion rate versus arc velocity. The arc velocities have been taken from averaging the values at every different concentration of  $\text{TiCl}_4$  to smooth the scatter inherent in the velocity measurements. The data are correlated as:

$$E = 155.02 \text{ Vel}^{-0.819} \quad (6-14)$$

where  $E$  is the erosion rate in  $\mu\text{g}/\text{C}$ . This agrees rather well with the experimental value obtained for copper erosion in nitrogen by Szente at relatively high velocities, i.e.

$$E \propto \text{Vel}^{-1} \quad (6-15)$$

Figure 6-14 Effect of Arc Velocity on Erosion Rate of Electrodes



$$Er = 155.02 * Vel^{-0.81944} \quad R^2 = 0.945$$

In Szente's case there was no chemical reaction to cause the erosion which was caused simply by the insufficient removal of heat from the cathode surface. The present analysis would suggest that even in the chemically aggressive atmosphere of  $TiCl_4$ , erosion rates are still primarily controlled by heat transfer and that the effect of titanium tetrachloride concentration is primarily to modify the arc velocity.

#### F. SEM Analysis

The Examination of the microstructure of TaC+Al material after tests were conducted with SEM (Scanning Electron Microscope). Figure 6-15 of the cathode inside surface (where the arc struck) and Figure 6-16 of the cathode outside surface (unaffected) show that the microstructure of the material was not visibly changed by the arc. In Figure 6-17 picked up close to the working surface of the cathode for run 9014, on the left, the upper and lower maps which were supposed to be black-white matched for unused electrodes show some porous spots (unmatched in black-white) indicating that aluminium has been removed. This implies that aluminium was preferentially consumed or evaporated at least initially. This difference in the erosion rates of aluminium and tantalum carbide and their variations with time could be two of the reasons responsible for the fluctuation of velocity and the scatter in the measured erosion rates .

In addition, it can be clearly seen in Figure 6-18 that some deposits containing titanium existed on the cathode surface, which is confirmed in the compositional analysis, as shown in Figure 6-19.

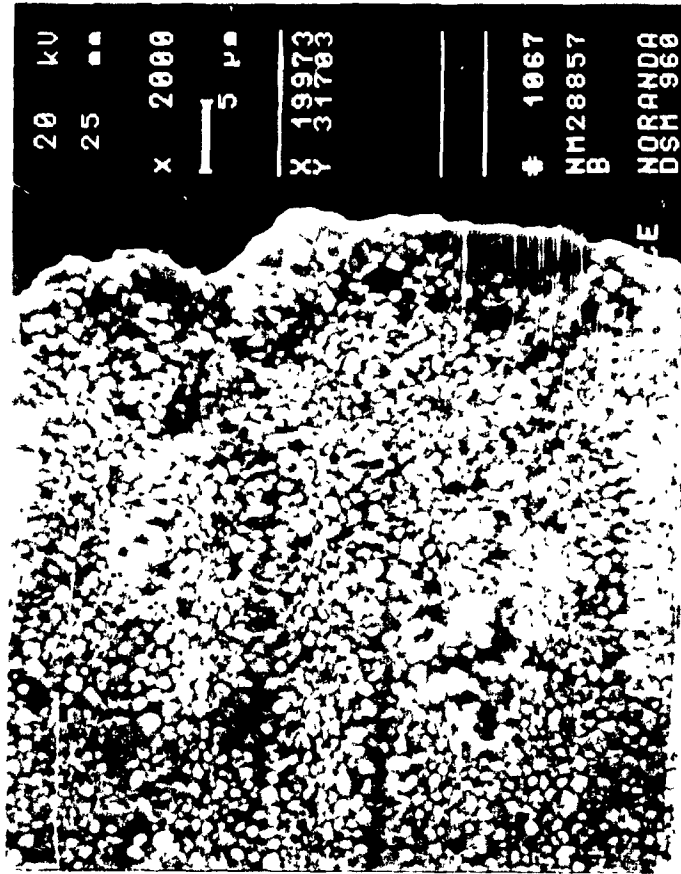


Figure 6-15 The Micrograph of the Cathode Inside Surface

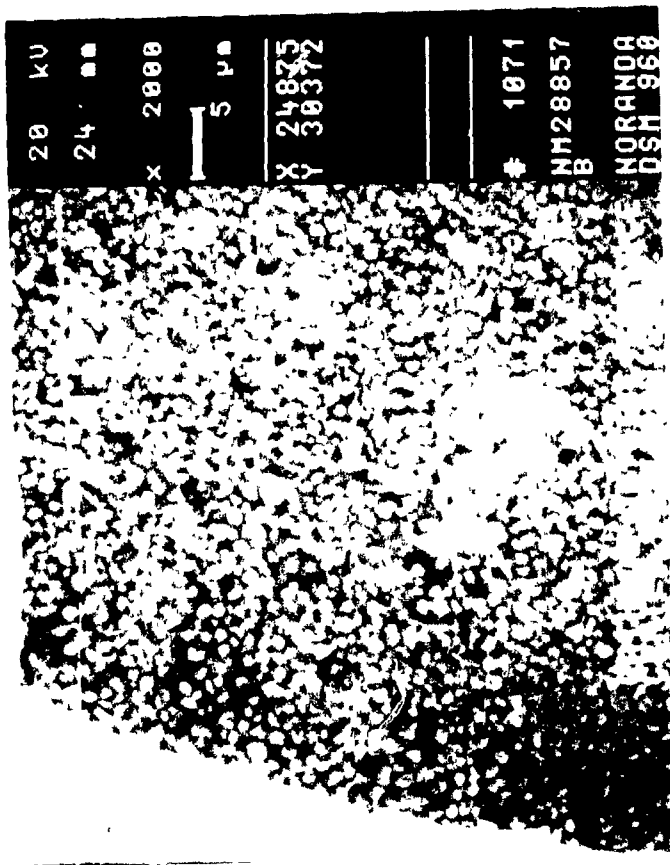


Figure 6-16 The Micrograph of the Cathode Outside Surface

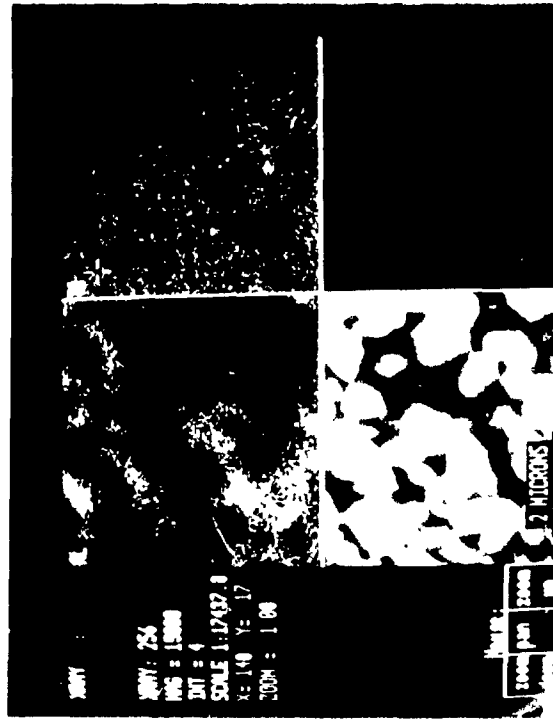


Figure 6-17 Comparison of Element Mapping on the Cathode Surface

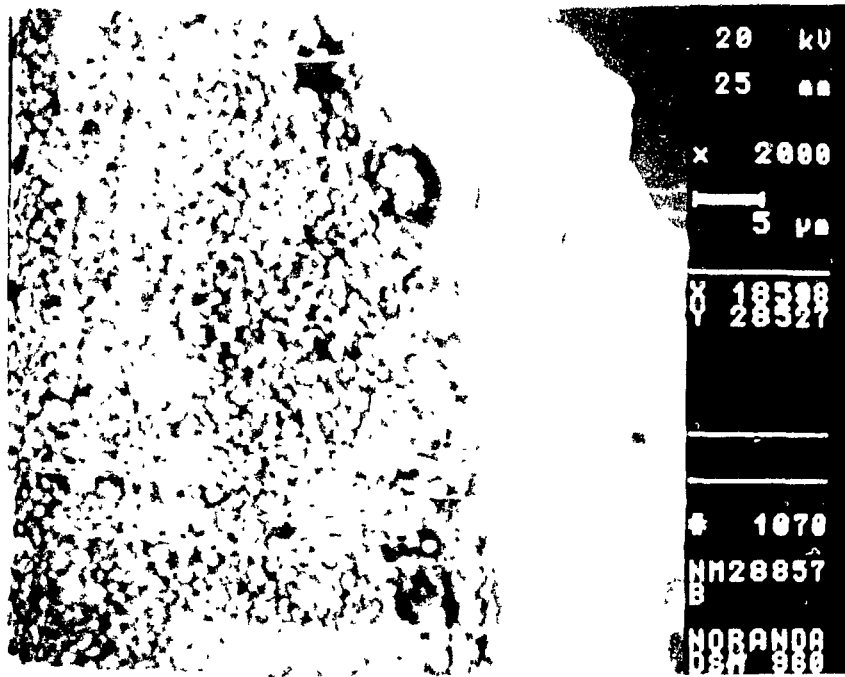
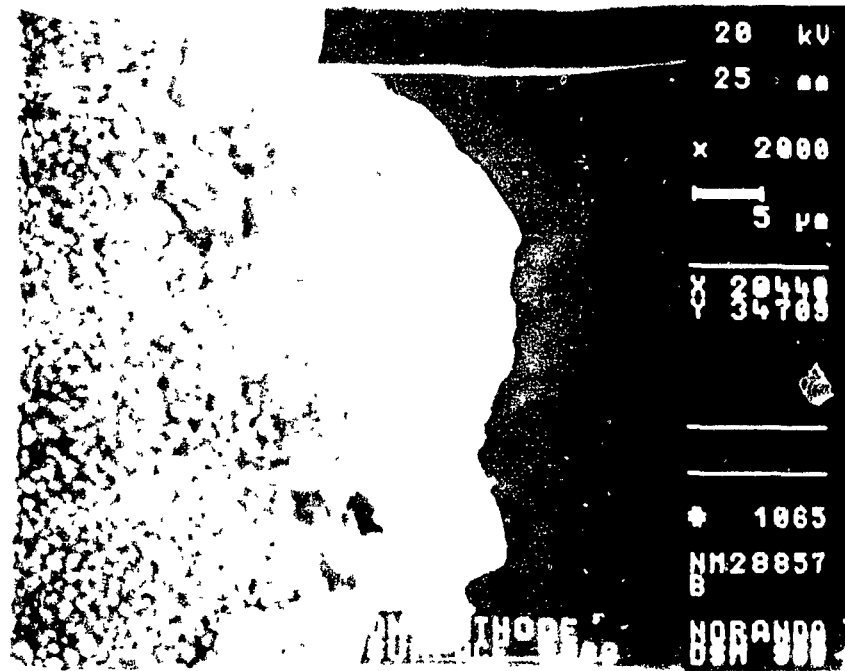


Figure 6-18 The Deposits of Titanium on the Cathode Surface

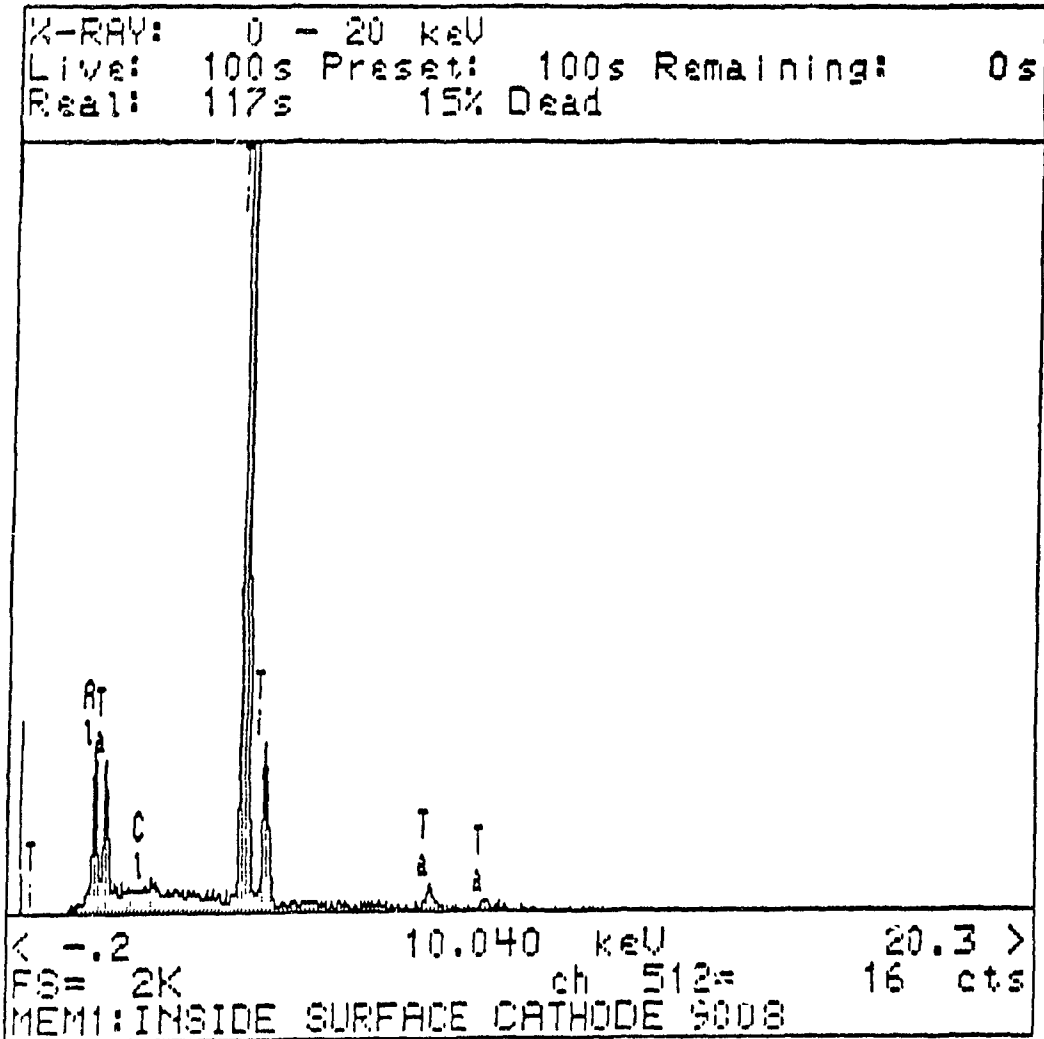


Figure 6-19 The Analysis of the Composition on the Cathode Surface

### G. The Behavior of the Anodes

Anode tips made of copper, tantalum and TaC+Al were used in this research. As was noted in the section on equipment, the copper anodes formed an integral part of the anode tube and so were cooled very well. They could not, however, be used with  $TiCl_4$  plasma gas because of the reactivity of copper with this chloride.

First TaC+Al and finally, pure Ta were used as the anode materials. Neither proved entirely satisfactory because of the way in which these anode tips were constructed and mounted on the anode holding tube. Since the tips were only press fit onto the anode tube, the thermal contact between the anode tip and the tube was not very good. The heating of the tips by the arc striking caused them to expand and thus further decreased the cooling efficiency. Quite the opposite was true of the cathode rings. Since these rings were mounted within the cathode holder, any expansion increased the tightness of the fit and reduced the thermal contact resistance. The eventual result is that the anode tips ran very hot leading to rapid evaporation of aluminium in the case of the composite electrodes and rapid attack of the tantalum at the higher temperatures. Although tantalum is resistant to chlorine at low temperature it is not inert.

The removal of aluminium by evaporation lead to the formation of a very brittle TaC anode tip. This was essentially inert to the titanium tetrachloride plasma but eventually failed by thermal stress and cracking. A photograph of a cracked anode is given in Figure 6-20. The material had lost the silvery appearance of the original TaC+Al and reverted to the dark brown color of the TaC. Because the tips tended to crack relatively large piece could fall off during operation; this explains the much greater scatter in the erosion measurements of the anodes reported in Table 6-7.

The much higher operating temperature of an anode tip, compared to the cathode ring, is shown in the photograph of the arc and electrodes in Figure 6-21 (Test No. 9027). In this figure, the anode is seen to be much brighter (the bright ring) than the cathode which is relatively well cooled. Similar photographs of an argon arc between

copper electrodes always show the anode completely dark while the cathode shows a single hot spot at the arc root.

In the type of plasma torches contemplated for use in any titanium production process, the cathodic erosion is always much more severe than the anodic erosion. Both electrodes would be in the form of an internally mounted rings and thus both could be well cooled. It may thus be concluded that the anomalously high anode erosions observed in this work are simply an artifact of the geometry and design chosen. The composite TaC+Al material should then be quite suitable as an anode material. Even tantalum might be suitable as an anode material provided that it is directly cooled and thus kept at temperatures where it is not attacked by the chlorine.

## H. Conclusions

i) The use of TaC+Al electrodes allowed the generation of stable plasmas in  $\text{TiCl}_4$  concentrations up to 30%. This limit was dictated by the temperature limitations of the cooling system (to avoid condensation of the  $\text{TiCl}_4$  gas) and the capacity of the feeding system but not the characteristics of the plasma. Operating voltage ranged from 35 to 62 volts for an arc gap of 4 mm and fluctuations in the voltage were in the range of 1-4 volts once the feeding system stabilized. The plasma current was extremely stable.

ii) The cathode erosion rates increased with increasing concentration of  $\text{TiCl}_4$  gas. This may have been because the arc velocity decreased due to gas density increases which accompanies the increase in  $\text{TiCl}_4$  concentration. The highest measured rates were less than 30 micrograms/C for a concentration of about 15%.



Figure 6-20 A Tantalum Carbide Anode Tip After Testing



Figure 6-21 A Photograph of the Arc in  $\text{TiCl}_4$  Gas

## CHAPTER 7.

### CONCLUSIONS AND RECOMMENDATIONS

---

#### 7.1 Conclusions

An experimental investigation was carried out to identify a suitable electrode material for the plasma treatment of titanium tetrachloride and to determine the behavior of the arc and the performance of the electrodes.

A DC plasma torch was modified and used for the study. Experimental techniques were developed to work with the highly corrosive and toxic  $\text{TiCl}_4$ . Experiments were carried out at 100 A, using a magnetic field of 1000 Gauss to rotate the arc. The pressure in the torch was kept constant at 1 - 1.1 atm and the temperature of the cooling water for electrodes was kept in the range of 358 - 363 K to avoid condensation of  $\text{TiCl}_4$  in the reactor. The flow rate of argon was fixed at 15 L/min and gaseous  $\text{TiCl}_4$  was added to this. The arc voltage, velocity and electrode erosion rate were measured as a function of  $\text{TiCl}_4$  concentration and test duration.

Pure sintered TaC was initially tried as electrode material. This cracked within seconds of operation even in pure argon due to thermal shock. It was determined that this brittle ceramic with relatively poor thermal conductivity could not be used. A composite material, TaC+Al was identified as a successful electrode material. Porous tantalum carbide infiltrated with Al is ductile and has a much higher thermal conductivity than the porous TaC alone and so can resist thermal shock for a prolonged time.

Stable DC plasma arc was produced with  $\text{TiCl}_4$  concentrations at up to 30 percent molar  $\text{TiCl}_4$  in argon for up to 20 minutes. The arc voltage with 4 mm interelectrode gap were in the range of 35-62 V with fluctuations in the range 1-4 V. Higher concentrations of  $\text{TiCl}_4$  were not used due to the limitations of the feeding

system and the need to keep the cooled electrodes above the dew point of the  $\text{TiCl}_4$ . The stable behavior of the arc at 30 %  $\text{TiCl}_4$  suggests that a pure  $\text{TiCl}_4$  plasma is feasible provided that a higher temperature cooling loop is used.

Arc velocities were about 13 m/s in pure argon; they increased as  $\text{TiCl}_4$  was added in low concentration and then decreased with increasing  $\text{TiCl}_4$  concentration, the latter effect can be attributed to changes in gas density. After an initial period of higher erosion, the erosion rates were independent of running time. Erosion rates increased with increasing  $\text{TiCl}_4$  concentration. The highest measured values were about  $30 \mu\text{g}/\text{C}$  at 14.3 %  $\text{TiCl}_4$ .

Anode erosion rates were higher but were an artifact of the geometry and design of the anodes used in this work. Anode erosion is not considered to be a major problem in an industrial torch.

## 7.2 Recommendations

According to experience accumulated in this experimental study it is found that in order to develop a stable and reproducible plasma torch for industrial production of titanium the behavior of the electrodes is a critical factor. The proposed TaC+Al, or some similar mixture of TaC which has similar thermo-mechanical properties, could be acceptable materials for electrodes of a DC plasma torch. However the following aspects should be considered:

- i) The initial porosity of the TaC and the aluminium infiltration procedure must be carefully controlled to produce electrode materials of reliable performance.
- ii) The design of the electrode cooling system is crucial to the successful production of pure  $\text{TiCl}_4$  plasmas. Condensation must be avoided but at the same time the electrodes must be cooled as well as possible.

## REFERENCES

---

- Apelian, D. & Szekely, J.** Editors "Plasma Processing and Synthesis of Materials", Symposium held April 21-23, 1987, Anaheim, Cal. USA, MRS 1987.
- Baddour, R.F. and Timmins, R.S.** "The Application of Plasma to Chemical Processing", MIT Press, 1967.
- Barksdale, J.** "Titanium - Its Occurrence, Chemistry and Technology", The Ronald Press Company, 1966.
- Bokhari, A. and Boulos, M.** "Energy Balance for a DC Plasma Torch", Can. J. of Chem Eng., 58, (4), 171, 1980.
- Bunting, K.A.** "Sodium and Titanium Tetrachloride Feed Systems for a Plasma Route to Titanium", ISPC-6, Montreal, July, 1983.
- Chen, F. F.** "Introduction to Plasma Physics", Plenum Press, 1974.
- Choi, H. K.** "Energy Distribution and Heat Transfer in an Argon Transferred-Arc Reactor", Ph.D Thesis, McGill U., 1981.
- Edels, H** "Properties and Theory of the Electric Arc", IEE, P. No..3498, Feb., 1961
- Farthing, T.W.** "Applications of Titanium and Titanium Alloys", Titanium-Science and Technology, Proc. of the 5th Intern. Conf. on Titanium, Sept., 1984, Munich, FRG, 1985.
- Francis, G.** "The Glow Discharge at Low Pressure", Encyclopedia of Physics, p. 53, 1956.
- Froes, F.H.** "Titanium Products and Applications", J. of Metals 39, 3, 1987.
- Gauvin, W. H., Drouet, M. G. & Munz, R. J.** "Development in Plasma Processes for Extractive Metallurgy", J of Metal, 1987.

- Guile, A. E.** "Arc-Electrode Phenomena", Proc. IEE, IEE Review, Vol. 118, No 9, Sept., 1971.
- Guile, A. E.** "Electric Arcs: Their Electrode Processes and Engineering Applications", IEE, Proceedings Vol. 131 Pt. A, No. Sept, 1984
- Habelrih, M.** "Electrode Erosion in Steam Plasma", M Eng. Thesis, Dept of Chem. Eng., McGill U., 1990.
- Hamblyn, S.M.L., Reuben, B.G., Thompson, R.** "Hydrogen Reduction of Boron Trichloride to Boron in a R.F. Plasma in Special Ceramics", British Ceramic Research Association, Vol. 5, p. 147,
- Hamblyn, S.M.L.** "A Review of Applications of Plasma Technology with Particular Reference to Ferro-Alloy Production", National Inst for Metal, Rep. No 1895, 1977.
- "Handbook of Chemistry and Physics"**, Robert C. Weast (ed), 58th edition, CRC Press, Inc., 1977-88.
- Hellund, E. J.** "The Plasma State", Reihold Publishing Corp, 1961.
- Ikeshima, T.** "Recent Developments in Titanium Sponge Production", Titanium-Science and Technology, Proceedings of the 5th International Conference on Titanium, Sept. 10-14, 1984.
- Ishizuka, R. and Akashi, K.** "The Formation of Titanium from Titanium Tetrachloride Introduced into an Argon Plasma Jet", J. of High Temp. (in Japanese), Sept., 1979.
- "JANAF Thermochemical Tables"**, D.R. Stull et all (ed), Clearinghouse for Federal Scientific and Technical Information 1960, 1965.
- Kettaini, M. A., et al** "Plasma Engineering", John Wiley & Sons, 1973
- Kovalenko, A. D.** "Thermoelasticity", Wolter-Noordhoff, 1969.
- Kupradze, V. D. Editor** "Three-Dimensional Problems of the Mathematical Theory of Elasticity and Thermoelasticity", North-Holland, 1979

- Laudau, L. D. & Lifshitz, E. M.** "Theory of Elasticity" Vol.7 Pergamon Press, (3rd Ed) 1986.
- Lewis, G.N. & Randall, M.** "Thermodynamics", McGraw Hill (2nd Ed) 1961  
Revised by **K. Pitzer and L.Brewer.**
- McQuillan, A. D., et al** "Titanium-Metallurgy of the Rower Metals-4", Butterworths Scientific Publications, 1956.
- McTaggart, F. K.** "Plasma Chemistry in Electrical Discharges", Elsevier Publishing Company, 1967.
- Mehmetoglu, T.** "Characteristics of a Transferred-Arc Plasma", Ph.D Thesis, Dept of Chem. Eng., McGill U., 1980.
- Miller, R.C., et al** "Reaction of Titanium Tetrachloride in a Radio Frequency Plasma Torch", I & EC. Process Design and Development, Vol. 8 No. 3, July, 1969.
- Munz, R. J.** "The Decomposition of Molybdenum Disulphide in an Induction Plasma Tail Flame", Ph.D, McGill U., 1974.
- Nicholson, D. R.** "Introduction to Plasma Theory", Jogn Wiley & Sons, 1983.
- Oskam, H. J.** "Plasma Processing of Materials", Noyes Publication, 1984.
- Petrunko, A. N.** "Status and Prospects for the Development of Titanium Sponge Production", Titanium-Science and Technology, Proceedings of the 5th International Conference on Titanium, Sept. 10-14, 1984.
- Perry, R. H. and Chilton, C. H.** Chemical Engineering Handbook, 5th Ed., McGraw-Hill Book Company, 1973.
- Reed, T.B.** "Introduction Coupled Plasma Torch", J. Appl. Physics, 32,821, 1961.
- Smith, A. and Adams, N. G.** "Elementary Plasma Reactions of Environmental Interest", Topics in Current Chemistry 89, Springer-Verlag, 1980.
- Szente, R. N., Munz, R. J. and Drouet, M. G.** "Effect of the Arc Velocity on the Cathode Erosion Rate in Argon-Nitrogen Mixtures", J. Phys: Appl. Phys. 20 (1987). Printed in the UK.

**Szente, R. N., Munz, R. J. and Drouet, M. G.** "Cathode Erosion in Inert Gases: The Importance of Electrode Contamination" *Plasma Chem. & Plasma Processing*, Vol. 9, No. 1, 1989.

**Szente, R. N., Munz, R. J. and Drouet, M. G.** "The Effect of Low Concentrations of a Polyatomic Gas in Argon on Erosion on Copper Cathodes in a Magnetically Rotated Arc", *Plasma Chem. & Plasma Process*, Vol.7, No.3, 1987.

**Szente, R. N., Munz, R. J. and Drouet, M. G.** "Arc Velocity and Cathode Erosion Rate in a Magnetically Driven Arc Burning in Nitrogen" *J. Phys. D: Appl. Phys.* 21 (1988) 909 - 913. Printed in UK.

**Szente, R. N., Drouet, M. G. and Munz, R. J.** "Method measure current distribution of an electric arc at tubular plasma torch electrodes" *Rev. Sci. Instrum.* 61 (4), April 1990.

**Szente, R. N.,** "Erosion of Plasma Torch Electrodes", PhD Thesis, October 1989

**Timoshenko, S. & Goodier, J. N.** "Theory of Elasticity", McGraw Hill, 1951.

**Tsantrizos, P. G.** "The Characteristics of Titanium Tetrachloride Plasmas in a Transferred-Arc Systems", Ph.D Theses, Dept. of Chem. Eng., McGill U., 1988

**U.S. National Materials Advisory Board** "Plasma Processing of Materials", Report No. NMAB-415, Washington, 1985.

**Yean, D.H. and Riter, J.R.** "High Temperature Heterogeneous Equilibriums in the Unit Activity Approximation II. Titanium Tetrachloride-hydrogen system", *Metallurgical Transactions*, Vol. 1, No. 5, 1974